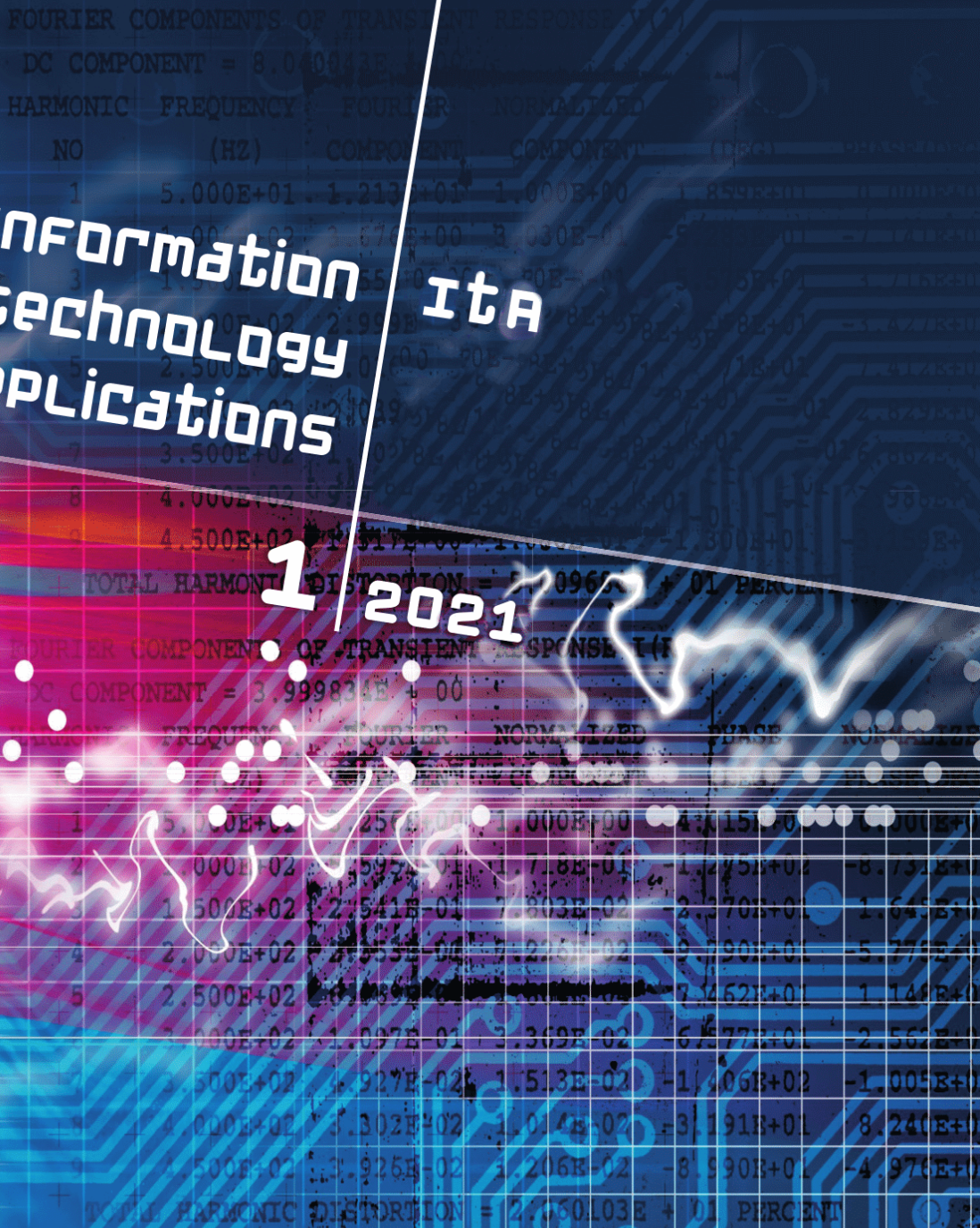


Information Technology Applications

1 2021





SLOVENSKÁ SPOLOČNOSŤ PRE KYBERNETIKU A INFORMATIKU PRI SAV
SLOVAK SOCIETY FOR CYBERNETICS AND INFORMATICS

International Journal of Information Technology Applications (ITA)

Volume 10, Number 1, September 2021

AIMS AND SCOPE OF ITA

The primary aim of the International Journal of Information Technology Applications (ITA) is to publish high-quality papers of new development and trends, novel techniques, approaches and innovative methodologies of information technology applications in the broad areas. The International Journal of ITA is published twice a year. Each paper is refereed by two international reviewers. Accepted papers will be available online with no publication fee for authors. The journal is listed in the database of the Russian Science Citation Index (RSCI). The International Journal of ITA is being prepared for the bibliographic scientific database Scopus.

Editor-in-Chief

prof. Ing. Štefan Kozák, PhD. Faculty of Informatics, Pan-European University in Bratislava
stefan.kozak@paneurouni.com

Executive Editor

Ing. Juraj Štefanovič, PhD., Faculty of Informatics, Pan-European University in Bratislava
juraj.stefanovic@paneurouni.com

Editorial Board

Ladislav Andrášik, *Slovakia*
Mikhail A. Basarab, *Russia*
Ivan Brezina, *Slovakia*
Yakhua G. Buchaev, *Russia*
Oleg Choporov, *Russia*
Silvester Czanner, *United Kingdom*
Andrej Ferko, *Slovakia*
Vladimír S. Galayev, *Russia*
Ladislav Hudec, *Slovakia*
Jozef Kelemen, *Czech Republic*
Sergey Kirsanov, *Russia*

Vladimir I. Kolesnikov, *Russia*
Štefan Kozák, *Slovakia*
Vladimír Krajčík, *Czech Republic*
Ján Lacko, *Slovakia*
Igor Lvovich, *Russia*
Eva Mihaliková, *Slovakia*
Branislav Mišota, *Slovakia*
Martin Potančok, *Czech Republic*
Eugen Ružický, *Slovakia*
Václav Řepa, *Czech Republic*
Jiří Voříšek, *Czech Republic*

International Journal of Information Technology Applications (ITA)

Instructions for authors

The International Journal of Information Technology Applications is welcoming contributions related with the journal's scope. Scientific articles in the range approximately 10 standard pages are reviewed by two international reviewers. Reports up to 5 standard pages and information notices in range approximately 1 standard page are accepted after the decision of editorial board. Contributions should be submitted via e-mail to the editorial office. The language of contributions is English. Text design should preserve the layout of the template file, which may be downloaded from the webpage of journal. Contributions submitted to this journal are under the author's copyright responsibility and they are supposed not being published in the past.

Deadlines of two standard issues per year

| | |
|---------------------------|-------------------------------|
| paper submission deadline | – end of May/end of October |
| review deadline | – continuous process |
| camera ready deadline | – end of June/end of November |
| release date | – Summer/Winter |

Editorial office address

Faculty of Informatics, Pan-European University, Tematínska 10, 851 05 Bratislava, Slovakia
juraj.stefanovic@paneurouni.com

Published by

Pan-European University, Slovakia, <http://www.paneurouni.com>

Paneurópska vysoká škola, n.o., Tomášikova 20, 821 02 Bratislava, IČO 36 077 429

Civil Association EDUCATION-SCIENCE-RESEARCH, Slovakia, <http://www.e-s-r.org>

OZ VZDELÁVANIE -VEDA-VÝSKUM, Andrusovova 5, 851 01 Bratislava,
IČO 42 255 180

Slovak Society for Cybernetics and Informatics (SSKI) at the Slovak Academy of Sciences,
Slovenská spoločnosť pre kybernetiku a informatiku pri SAV (SSKI),
Ústav automobilovej mechatroniky, Fakulta elektrotechniky a informatiky STU,
Ilkovičova 3, 812 19 Bratislava 1, IČO 00 178 730, <http://www.sski.sk>

Electronic online version of journal

<http://www.paneurouni.com/ITA>

<http://www.e-s-r.org>

visit Archive and Instructions for authors:

Print

Multigrafika s.r.o., Rajecká 13, 821 07 Bratislava

Subscription

Contact the editorial office for details.

Older print issues are available until they are in stock.



ISSN: 2453-7497 (online)

ISSN: 1338-6468 (print version)

Registration No.: EV 4528/12



Contents

Editorial

| | | |
|---|---|----|
| ▶ | PREDICTIVE INTELLIGENT MAINTENANCE CONTROL USING AUGMENTED REALITY Michal Kostoláni, Justín Murín, Štefan Kozák | 3 |
| ▶ | AN APPLICATION FOR OPTIMAL MATERIAL FLOW IN INDUSTRIAL WAREHOUSES Filip Žemla, Ján Cigánek | 13 |
| ▶ | PROBLEMS OF DATA TRANSFER IN THE NETWORK OF THE ORGANIZATION WITH MINIMIZED CAPABILITIES OF THE USED RESOURCES Andrey Preobrazhenski, Igor Lvovich, Yury Preobrazhenski | 25 |
| ▶ | COMPARISON AND ANALYSIS OF THE USE OF ADVANCED METHODS OF ARTIFICIAL INTELLIGENCE FOR NEURODEGENERATIVE DISEASES Eugen Ružický, Štefan Kozák, Ján Lacko, Juraj Štefanovič, Alfréd Zimmermann, Milan Rusko, Petra Brandoburová, Matej Škorvánek | 35 |
| ▶ | STATISTICAL MECHANICS OF COMPLEX GRAPHS David Šablatúra | 47 |
| ▶ | MODEL PREDICTIVE CONTROL - APPLICATION FOR PHYSICAL MODEL Štefan Kozák | 67 |
| | List of Reviewers | 77 |

Editorial

.....

Greetings from the desk of the Editor-in-Chief

It is a great honor and privilege for me to be appointed as Editor-in-Chief of the International Journal of Information Technology Applications (ITA). Journal ITA is an official journal published by the Faculty of Informatics of the Pan-European University on behalf of Slovak Society for Cybernetics and Informatics, which is one of the national scientific societies at the Slovak Academy of Sciences and on behalf of the civil association EDUCATION-SCIENCE-RESEARCH.

The journal publishes articles investigating the design, simulation and modeling, implementation and analysis of advanced methods, algorithms and technologies in different fields of applications, for example in industries, economy, health care and services, etc.

This journal aims to integrate the latest knowledge and practical results from researchers, educators and practitioners who effectively use the knowledge and bring it to practical life. Submissions of original research and focused review articles are welcomed from scientists and engineers across the community.

I would like to thank my predecessor, the former Editor-in-Chief prof. Frank Schindler and his team. I applaud him for his inspiring commitment, outstanding contribution, and service in elevating the journal to its current level of excellence.

I assume and consider it necessary in the nearest future to expand the editorial board with new members who have significant results in the subject area. The new editorial team will continue to seek his expert guidance for taking IT to further heights of recognition and readership.

As I look forward to this new role, I welcome input from you, our readers and contributors to enhance the overall quality of our journal. Together with the erudite team of editorial board, I will work passionately to take the journal to the next level. Editorial board team welcomes your manuscript submissions and looks forward to an enjoyable experience while working with your contributions.

With best wishes for a very happy and successful 2022.

Štefan Kozák
ITA Editor-in-Chief

Dear authors, dear readers,

this issue is completed after the second half of season 2021, the second season of epidemic situation which reduced direct communication where new ideas and activity mostly reveal. Up to date, we have collected six papers containig various topics in information technology and theory.

Besides two present publishers of our ITA journal, Pan-European University and the civil association EDUCATION-SCIENCE-RESEARCH, a third subject expressed interest and joined this season being a co-publisher: Slovak Society for Cybernetics and Informatics (SSKI) at the Slovak Academy of Sciences. This is a promise for more support of ITA journal activity in the near future.

Despite of contemporary complicated period, our Faculty of informatics has a constant interest from young graduated as well as older employed people to enter our study program. We offer a space in our journal to publish interesting results from their qualifying theses and assignments.

Besides of two promised issues of journal a year, we would like to produce in the future some additional issues covering selected professional events. Another special attempt is to produce monotematic editions of journal, after the negotiation with joined communities of experts. Your forthcoming papers and contributions are welcomed around the year.

Juraj Štefanovič
ITA Executive Editor

PREDICTIVE INTELLIGENT MAINTENANCE CONTROL USING AUGMENTED REALITY

Michal Kostoláni, Justín Murín, Štefan Kozák

Abstract:

Modern manufacturing industry is currently facing significant challenges regarding the concept of Industry 4.0. The promise of increased productivity and flexibility in manufacturing processes cannot be achieved without implementation of systems and advance methods based on smart technologies. Implementation of Industrial Internet of Things (IIoT), Condition Monitoring, Big Data, Cloud computing, virtual and augmented reality in maintenance processes will significantly increase the effectivity and quality of manufacturing processes as well as eliminate the human factor. Under this perspective, cyber-physical systems can be accessible from remote location; process parameters can be visualized at real time and prediction of unexpected production stop due to machine breakdown will be significantly reduced. The paper deals with the development of effective approach to real-time process control using parameters visualization of manufacturing process with the use of augmented reality smart glasses. Collected data from condition monitoring sensors from electric monorail system are evaluated in real time and visualized in the field of view of maintainer. Critical values from field of sensors are highlighted and enable to predict manufacturing breakdown. On real example from automotive industry will be demonstrated the signification and effectivity for maintenance of electric monorail system and potential for application in different types of modern industrial processes with the focus on rule-based intelligent predictive maintenance control.

Keywords:

Industry 4.0, intelligent control, smart maintenance, augmented reality, condition monitoring, cyber-physical systems.

ACM Computing Classification System:

Embedded and cyber-physical systems, Real-time systems, Communication hardware, interfaces and storage.

Introduction

Industry 4.0 represents the fourth industrial revolution in manufacturing industry with the focus on the establishment of intelligent product and production processes. The promise of increased productivity and flexibility is a current driving force at the heart of the industry development representing the realization of large-scale changes in current industrial manufacturing. These changes include automation, digitalization, intelligent control methods and integration of information and communication technologies (ICT) at all levels of prototyping, process control, maintenance and services. These challenges cannot be achieved without the implementation of systems and methods based on smart manufacturing and smart maintenance. Systems and methods such as Internet of Things, Cyber-physical systems, Big Data, Cloud computing, virtual and augmented reality refer to the methodology of Industry 4.0 to achieve demand of increased flexibility and performance of production.

[1]

The internet of things (IoT) is an information network of physical objects (sensors, machines, car, buildings, and other items), that allows interaction and cooperation of these objects to reach common goals. Term IoT affects among others transportation, healthcare or smart homes, the Industrial Internet of Things (IIoT) refers to industrial environment. Application of IIoT provides to internet-enabled cyber-physical systems ability to connect to new interconnection technologies and applications. Based on this perspective, industrial cyber-physical systems can be accessible from remote locations, process data on them can be processed, transformed, analyzed and managed in distributed locations at real time. [1, 2]

Over the last years, the initiatives to apply smart manufacturing and maintenance methods and systems based on interoperability, virtualization, decentralization, modularity and real time data collection and analysis to improve performance, intelligence, cyber security and compatibility has increased dramatically.

Concept of smart manufacturing and maintenance referred to Industry 4.0 is characterized by and based on the following technologies (Fig.1):

- a. *Autonomous Robot* that can interact with one another. These robots are interconnected so that they can work together and automatically adjust their actions to fit the next unfinished product in line. High-end sensors and control units enable close collaboration with humans.
- b. *Big Data* - data collection and analysis refers to a large amount of diversified time series generated at a high speed by equipment. Smart manufacturing requires data to be collected and analysed at real time. Based on the information collected, real-time intelligent control and decision-making methods can be used for support of manufacture and maintenance processes.
- c. *Cloud Computing* is shared pool of configurable computer system resources and higher-level services that can be rapidly provisioned over the internet.
- d. *Industrial Internet of Things* refers to an industrial framework whereby large numbers of devices or machines that are connected and this enables intelligent industrial operations using advanced data analytics.
- e. *Cyber security* with the increased connectivity and use of standard communications protocols that come with Industry 4.0, the need to protect critical industrial processes, the process of keeping every industrial layer, including SCADA servers, HMI, engineering workstations, PLCs, network connections and people guarded against cyber threats without impacting on operational continuity and the consistency of industrial processes.
- f. *Augmented (AR) and Virtual Reality (VR)* technologies are increasingly being used in manufacturing processes. These use real and simulated objects and information to create a simulated environment and digital information that can be used to enhance the manufacturing and maintenance processes, qualification and eliminate the human factor.

The paper consists of three parts. The part 1 deals with problem formulation of current state of maintenance, industrial internet of things and industrial augmentation. The part 2 of the paper provides a description of the proposed approach and system implementation in terms of the hardware and software components. The part 3 deals with the case study of possibilities and new methodology of augmented reality in industrial application.

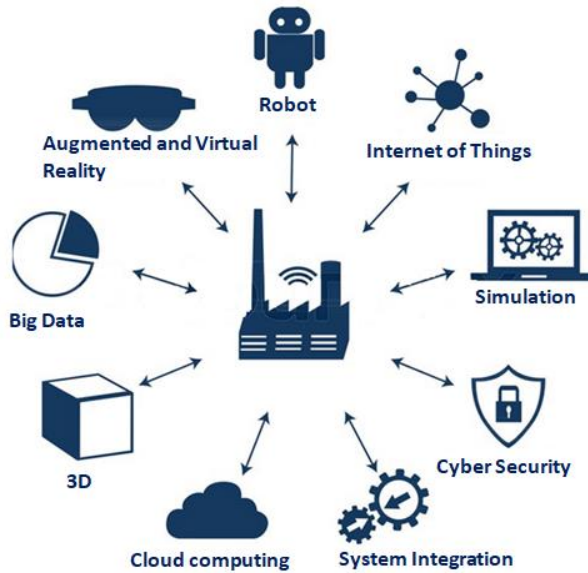


Fig.1. Basic scheme of the technologies in smart factory.

1 Problem Formulation

The paper proposes a new visualization approach of process equipment parameters in automotive manufacturing using augmented reality. This approach aims at providing support to the maintenance worker through visualization of different information, originating from condition monitoring system.

Maintenance is a strategic concern when developing and manufacturing a product. Breakdowns and unexpected production stops are expensive, because of financial and operating time losses. For product manufactures, preventive maintenance and asset repairs consume unnecessary resources, operational and service cost, and present a serious impediment to efficient operations. [3, 5]

The term Industry 4.0 arises from the combination of new information technologies and data analysis with advanced fabrication techniques and processes. To accomplish demands of Industry 4.0, Industrial Internet of Things represents a superior approach that involves continually generating and transmitting machine behaviour data, capturing the data in a central repository and applying advanced big data analytics techniques to sort through massive amounts of data and identify important patterns to deliver predictive maintenance insights. This significant approach becomes relevant only in case of displaying the correct data in the correct place and it can lead to just in time maintenance and increase product uptime, improve asset efficiency and eliminate unnecessary repair costs. The key enabler for smart maintenance is the ability to interact with in real time, and expand the capabilities of the physical world through computation, digitalization and visualisation with digital content. Comparison of traditional and smart maintenance approach is listed in (Tab.1)

Augmented reality (AR) refers to a new generation of systems with integrated computational and visualisational capabilities that combines real and virtual objects in a real environment. Industrial Augmented Reality (IAR) applications are systems to be used in a product lifecycle process utilizing the concept of spatially aligned and interactive overlay of computer generated information in a working context. [2, 4]

In context of rule based predictive maintenance, the AR application implements three main functionalities:

- Support through the visualisation of different types of information, as assembly sequence, spare parts and data from condition monitoring system.
- Maintenance process information provision in real time through instruction list.
- One point maintenance lessons to support maintenance worker through virtual demonstration, videos and image.

Table 1. Comparison of maintenance approach.

| Process | Traditional maintenance | Smart maintenance |
|-------------------------|--|--|
| Learning new technology | - Limited resources - Not up to date observations - Verbal guidance | - Learning by virtual and augmented reality - One point lesson - Digital guidance |
| Work execution | - Detailed work instruction missing - Paper documentation - Complicated remote worker assistance | - Real time support (text, voice, video) - Digital documentation - Hands free application - Online remote support |
| Work reporting | - Paper based orders and reports - Manual entry to company IT system | - Smart glasses connected to ERP System - Photo and video reports - Digital analysis |

2 System Implementation

The proposed approach aims at providing intelligent predictive maintenance control through the visualization of different types of information using augmented reality. For effective Industrial augmented reality applications is essential to display real data in the correct place. In this context, following essential components are needed (Fig.2): [6]

- Application that contains applications logic and controls access to database.
- Tracking that determines position and orientation of user and objects.
- Interaction registers and processes user input.
- Presentation, that generates and presents the AR scene through 3D visualization.
- Context collects contextual data and makes it available to other subsystems.
- World model contains information about real and virtual objects in the user environment.

Interaction between real and virtual objects is performed through AR marker (tag) that enables to attach information to real world facilities, assets, and objects, to provide just in place data. Tag enables digital information to flow from existing systems, such as condition monitoring or SAP for asset management and performance data, into the real world. Collection of tags related by a physical area is defined as a workspace. Each workspace is identified by unique selector and is aligned with physical world by landmark.

Augmented reality applications in automotive industry focus on all processes relevant to maintenance. After analyzing the state of the art and processes directly on the production lines, the pilot project was selected for the visualization of the operating parameters, instruction list and one point lesson. Data from field of sensors (temperature, vibrations, etc.) installed on the car transport system engines are dynamically processed and displayed to the maintenance worker in order to detect anomalies and more accurately identify possible sources of problems. Maintenance instruction lists and one point lessons guide are loaded from SAP system in real time and displayed in the smart glasses.

In order to develop the application for the cases described above, the proposed IAR system makes use of the fog computing communications architecture depicted in (Fig.3). Fog computing extends cloud computing by moving part of the computational and communication capabilities of the cloud close to the sensor nodes. Such an approach makes it possible to minimize the delay, which is a critical factor in dynamic systems of expanded reality. No less important is the distribution of computational power.

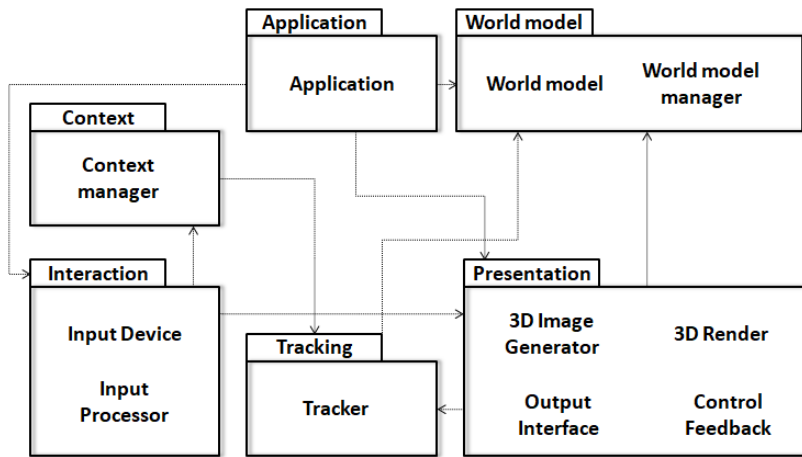


Fig.2. Reference architecture of IAR system.

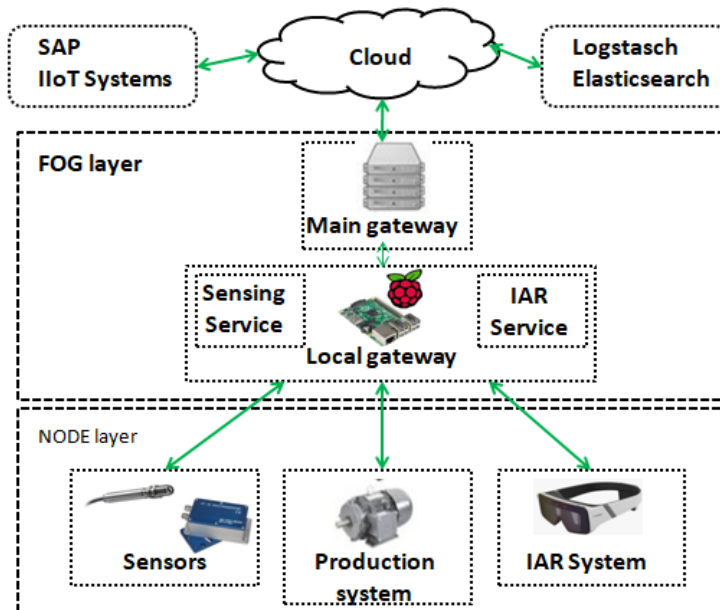


Fig.3. Fog computing communication architecture for IAR system.

The architecture of the proposed system is composed of the following layers: [4]

- Node layer includes all the IAR devices that interact with the services provided by the fog layer. The fog layer also exchanges data with sensor networks.
- Fog layer, which consists of dedicated computers that act as gateways and provides fog services.
- The cloud, which represents the place where the data is stored, analyzed and evaluated on receipt from multiple sources.

The communications between each IAR device and the fog layer are performed through Wi-Fi connections.

3 Case Study

The case study tested by this application originates the automotive industry maintenance and has been applied to the electric monorail system shown in (Fig.4) that transports car parts or bodies between assembly positions. An electric monorail system is a rail-bound type of conveyance with individually driven vehicle, which move independently on the closed rail system. This system consists of conductor rail, frame, engine, control unit, optical sensor and rolling wheel. Failure of any components in closed rail system cause interruption of production for several hours. [3]

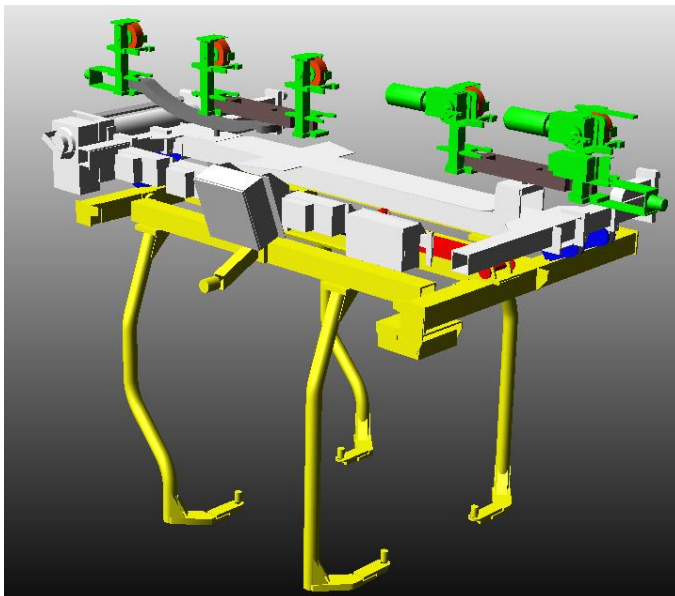


Fig.4. Electric monorail system.

To realize intelligent predictive maintenance control of electric monorail system using augmented reality, system according to the (Fig.3) was realized. The first layer represents smart glasses for augmented reality, electric monorail system and condition monitoring filed of sensors. The second layer is represented by Raspberry Pi 3 and the RAY-X datalogger. The third layer implementation enables device monitoring in real time, using an open Logstash server that allows data collection and transformation into JSON format and subsequent data transmission.

The search and analytics tool Elasticsearch enables you to search and analyze large amounts of data quickly and in real time. Subsequent visualization of operating statuses form condition monitoring, instruction lists and one-point lessons from SAP system is possible on a computer using the Kibana visualization program, or directly by using smart glasses for augmented reality. We propose the basic structure for intelligent predictive maintenance control using augmented reality according to the scheme shown in (Fig.5).

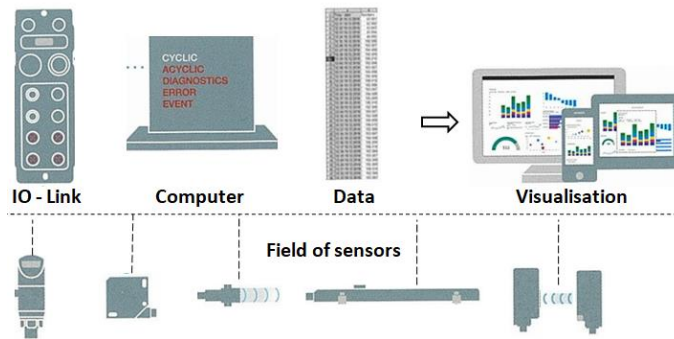


Fig.5. Scheme of intelligent predictive maintenance control.

In the application, which runs in augmented reality smart glasses, is the interaction between real and digital content performed through AR marker (tag). Workspace “Predictive maintenance of electric monorail system” was created and defined with unique selector and landmark in identical area to the physical location of the field of sensors. Once the workspace has been created, the individual digital tag is located in the space so that the information displayed in them complies with the requirements. For each tag, the source and path of the information (URL) to be displayed need to be defined, as well as the type of visualization. For better clarity, each description, picture, and status are assigned to each digital tag (Fig.6). The maintenance worker can visualize current and historical values from condition monitoring system in real time and just in place. Critical values from filed of sensors are highlighted and enable intelligent predictive maintenance control using augmented reality.



Fig.6. Realization of intelligent predictive maintenance control of electric monorail system using augmented reality.

Conclusion

This paper presented an intelligent approach to predictive maintenance control using augmented reality smart glasses to support maintenance worker in automotive industry. Multiple functionalities involving the visualization of different types of production related data, instruction lists and one-point lessons have been implemented in this direction. From experimentally achieved results compared with preventive maintenance approach is evident significant improvement in following aspects:

- Increased quality of maintenance processes.
- Increased failure prediction.
- Reduction of unexpected production stops.
- Elimination of human factor.

Further research should focus on the integration of augmented reality systems to existing multilevel control structures and extension of the application functionalities (visualization without landmark, spare parts control and documentation).

The proposed methodology can be used for the predictive maintenance control of robotics, conveyors and other mechatronics systems in industry (automotive, aviation, biotechnology etc.)

Acknowledgement

This paper is supported by the Scientific Grant Agency of Ministry of Education, Science, Research and Sport of the Slovak Republic, grant No. VEGA: 1/0102/18 and the APVV - 0246 - 12.

References

- [1] Kozák, Š., Ružický, E., Štefanovič, J., Schindler, F., Kozáková, A. (2018) ICT and control for Industry 4.0. In Páleník, T., Štefanovič, J. *AIFICT 2018: 1st International conference on applied informatics in future ICT*. Bratislava, Slovakia, pp. 7-13.
- [2] Kučera, E., Haffner, O., Drahoš, P., Kozák, Š. (2018) Emerging technologies for Industry 4.0: OPC unified architecture and virtual / mixed reality. In Páleník, T., Štefanovič, J. *AIFICT 2018: 1st International conference on applied informatics in future ICT*. Bratislava, Slovakia, pp. 57 - 62.
- [3] Kostoláni, M., Murín, J. (2018) Condition monitoring of electric monorail system in automotive industry. In Kozáková, A. *ELITECH'18: 20th Conference of doctoral students*. Bratislava, Slovakia, ISBN 978-80-227-4794-3
- [4] Blanco-Novoa, Ó. Fernández-Caramés, T.M., Fraga-Lamas, P., Vilar-Montesinos, M.A. (2018) A Practical Evaluation of Commercial Industrial Augmented Reality Systems in an Industry 4.0 Shipyard, *IEEE Access*, pp. 8201–8218.
- [5] Fernández del Amo, I., Erkoyuncu, J.A., Roy, R., Wilding, S. (2018) Augmented Reality in Maintenance: An information-centred design framework, *Procedia Manufacturing*, pp. 148–155.
- [6] Quandt, M., Knoke, B., Gorltd, C., Freitag, M., Thoben, K.-D., (2018) General Requirements for Industrial Augmented Reality Applications, *Procedia CIRP*, pp. 1130–1135.

▲ Authors

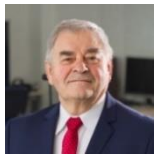
Ing. Michal Kostoláni, PhD.

young research and application scientist in the field of Industry 4.0 with a focus on modern methods of predictive maintenance for the automotive industry.
Faculty of Electrical Engineering and Information Technology,
Slovak University of Technology in Bratislava
Bratislava, Slovak Republic
michal.kostolani@stuba.sk



Prof. Ing. Justín Murín, DrSc.

currently the Head of the Department of Applied Mechanics and Mechatronics and Deputy Director of the Institute of Automotive Mechatronics at FEI STU. His basic research is mainly devoted to the development of new mathematical-physical material models and new finite element models for the analysis of mechanical, electromechanical and micro-electro-mechanical elements and systems made of traditional, but especially of functionally graded and multifunctional materials. In applied research he is engaged in numerical analyses of real systems of applied mechanics, mechatronics and electrical power engineering.
Faculty of Electrical Engineering and Information Technology,
Slovak University of Technology in Bratislava
Bratislava, Slovak Republic



prof. Ing. Štefan Kozák, PhD.

currently at the Institute of Applied Informatics at the Faculty of Informatics, Pan-European University in Bratislava. His research interests include system theory, linear and nonlinear control methods, numerical methods and software for modeling, control, signal processing, IoT, IIoT and embedded intelligent systems for digital factory in automotive industry.
Faculty of Informatics, Pan-European University, Bratislava, Slovakia
stefan.kozak@paneurouni.com

AN APPLICATION FOR OPTIMAL MATERIAL FLOW IN INDUSTRIAL WAREHOUSES

Filip Žemla, Ján Cigánek

Abstract:

The aim of the paper is to design and to create an application in the selected visualization environment, which will be used to simulate the movement of material in industrial warehouses. After entering the input data, the application automatically suggests the optimal way to store packages in the warehouse. The paper will describe the storage systems, database systems and relation database model used in the application. The visualization systems are introduced here, where the Promotic system will be presented and the development of practical result. The last part of paper describes the developed application and its functions.

Keywords:

SCADA systems, optimization, material movement, dynamic programming.

ACM Computing Classification System:

Information systems, data management systems, database management system engines, database views.

▀ **Introduction**

A SCADA system (Supervisory Control And Data Acquisition) is an architecture of control systems, consisting of computers, a communication infrastructure and a graphical interface. Their functions are to supervise management, data collection and the provision of a clear user environment. SCADA systems are used mainly in industrial production, but also in distribution and transport networks.

In storage systems, the material flow is increased; therefore it is necessary to ensure its fluidity in the shortest possible time. Today, there are many methods to increase efficiency, but their implementation is technically and financially demanding and is therefore only required in larger warehouses. In this work we therefore deal with the optimization of material movement in the SCADA system environment.

The aim of this work is to design an application in a SCADA system with decentralized control to display the optimal path of material movement. The optimal path will be designed for loading and unloading packages in a simulation warehouse with six racks. If a suitable location is found, its weight, dimensions and the current position of the user will be taken into account. If the packages are removed from storage, the closest package from the current position of the user will be found.

1 Storage systems

One of the main components of the modern logistics center infrastructure is the warehouse. In the logistics center, the warehouse serves as a distribution center, so its task is to receive and dispense pallets. The warehouse in the logistics center, as opposed to the warehouse in the production process, is focused on maximizing profit by satisfying customers' transport requirements. There are many storage systems, the use of which depends on the method of storage and the equipment used in the warehouse. We also select the storage system according to the type of stored material, its dimensions, weight and storage time. In our case we will use Pick-to-Light and Put-to-Light systems [7, 8].

The Pick-to-Light system is one of the modern material retrieval systems, significantly increasing the productivity of order fulfillment and at the same time reducing operator errors. It eliminates the need for paper expenses, removal orders and assembly sheets. This system also uses light sensors located in the racks to navigate the operator. After entering the shipment number into the system, the sensor lights up above the package, signaling the storage location with the specified quantity for the operator. **The Put-to-Light system** is based on the same principle, with the difference that the entered quantity is subtracted (selected) from the entered storage [5, 9, 10].



Fig.1. Warehouse using Pick-to-Light and Put-to-Light systems [4].

2 Database systems

The program system can be called a database system if two criteria are met. The first criterion is the ability to manage persistent data and the second is the ability to process large amounts of data efficiently. From these requirements, we can define a database system as a software system that is adapted to the efficient storage, selection and manipulation of large amounts of persistent data. Persistent data persists in the system for a long time, regardless of the programs used. Database systems work with data stored in a database, so its main functions are [2]:

- inserting new, empty files into the database,
- inserting data into an existing file,
- selection of data from an existing file,
- correction of data in an existing file,
- deleting an existing file from the database,
- deleting data from an existing file.

The database is an organized collection of data in electronic form. It is a set of structured, interrelated data grouped together, without unnecessary redundancy. A database consists of schemas that represent a set of data describing a database data model, which is a table. The tables represent an array of $n \times m$, where n is the number of columns and m is the number of rows. The table column defines the data name and data type. The most used data types in databases are numeric, date or logical [11].

The relational database model is currently a unified way of representing data at the logical level due to the simplicity that facilitates data representation. This database model is used in most popular database applications, such as Microsoft SQL Server, Oracle Database, MySQL, IBM DB2 or Microsoft Access [3].

Microsoft Access is a database management system from Microsoft. It offers a combination of graphical user interface and application development tools with the Microsoft Jet relational database engine. Microsoft Access can create tables and forms, as well as create complex queries without requiring any programming skills of users. Thanks to this feature, it deserved a place in the Microsoft Office package. Microsoft Access works with relational databases, saving them in its own file with the *.accdb* extension. In older versions, the *.mdb* extension was used [1, 14].

Microsoft Access is complemented by other services from Microsoft that allow the database to be stored in the cloud, backed up and encrypted. An interesting feature is that Access is so compatible with competing databases that it can work with data from Oracle databases. From the information obtained so far, it may be obvious that it can also communicate with other software from Microsoft, Microsoft SQL Server. As this application is available for students in the student version and sufficient to work with data in our work, it will be used to create a database and its subsequent connection with the visualization program Promotic [1, 14, 18].

3 Visualisation Systems

Visualization systems are responsible for consistent data display. All data must be sufficiently visible in compliance with ergonomic rules and psychological requirements. This means that the work environment in which the data is displayed must be configured and customized [15]. The ideal interface is clear, transparent and unobtrusive as little as possible. It allows the user to focus on process control without drainage attention to its very appearance [16].

SCADA systems consist of three components, namely a **PLC**, a **main station** with HMI and a **communication structure**. The PLC reads the values, which are then sent to the main station via the communication structure. The main station displays the received values to the operator in graphical and numerical form via the HMI. It is also possible to control these values after entering a value by the operator. The station sends a signal to the PLC, which sets the process to the desired behavior. Such systems are used mainly in industrial production halls, but nowadays they are also used in Smart home technology or Web technologies due to the possibility of remote access [15].

Promotic is SCADA / HMI system for creating applications in industrial automation. The Czech company MICROSYS created Promotic system with its operations and functions in 1991. Today, Promotic is one of the most widely used SCADA systems in the world. It deserved this award thanks to Promotic team's direct attention to the quality of services they provide to the customer. This means that they are constantly developing their product in the form of new versions, the current version is 9.0.8. It also contains rich documentation and provides top technical support.

As Promotic is constantly evolving, the features it provides are also being added. Promotic can access databases from the simplest ones such as Microsoft Excel or Microsoft Access to Oracle, MySQL and Post-greSQL databases [17, 18].

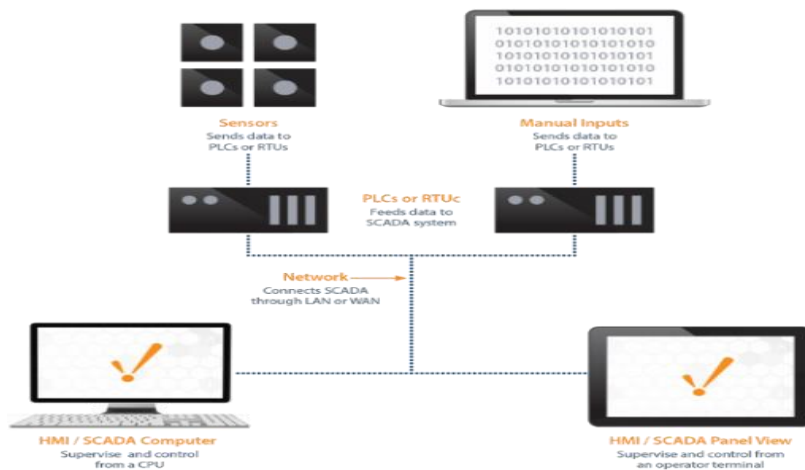


Fig.2. Diagram of SCADA systems [13].

It has also adapted to the needs of users for remote access by adding a Web server feature. The web server provides application conversion to HTML, XML, PHP and JS files for Internet browsers. Data transfer is based on the standard HTTP protocol and access to the application is handled by a secure login. Promotic system supports work with two scripting languages, VBScript and JavaScript. We use VBScript for local applications and JavaScript for the mentioned Web applications. In this work, we decided to use Promotic application using both programming languages [6, 17].

4 Case Study

The aim of the application is to streamline the storage and retrieval of packages in the warehouse. This is achieved by using dynamic programming, looking for the shortest way to save the package. In the application, we used an imaginary, presentation warehouse consisting of six shelves. Each of the shelves is divided into two sides, each side having two shelves and 20 segments, places where packages can be stored.

The application consists of two main parts, according to which the job description will be divided. The first part is a description of the tables used in the database and their connection with the visualisation application Promotic. The second part is a description of the HMI application, in which the functionalities of the elements are described. The HMI application was created in accordance with the IEC 73 standard.

a) Database

An important part of the application is the database, which is divided according to the use of variables into tables. All tables were created and managed in the MS Access environment.

The Segments table contains the properties of all segments in the warehouse, where the segment number (attribute “Segment” in the database) is the primary key with unique values. The second table is **the package table**, in which the values entered by the user in the application are written. Each entity corresponds to one package and attributes.

The next **table** is for **user management**, each user having the attributes of his ID, which serves as the primary key, login name, password, access level, and default user language. The access level corresponds to the function of the user in the warehouse. Users with an access level corresponding to 2 are allowed to load and unload packages from the warehouse with the shortest route displayed. Users with access level value 1 do not have permission to insert and unload packages, and the shortest path will be displayed after entering input values to other users with access to package manipulation in the database. The Language attribute numerically represents one of the seven languages that can be selected in the application.

The distance table and **the neighbour table** serve as two-dimensional arrays of the properties of individual nodes. Both tables have 21 attributes, with the first attribute indicating information for which node the entity is. Other attributes indicate how it relates to a given node. In the case of a distance table, this is the distance of the node to which the entity belongs to the given node to which the attribute corresponds. And in the neighbors table as in the previous table, but instead of the distance, the cell informs about all the neighbors of the entity node.

b) Dynamic Programming

Dynamic programming is one of the most commonly used methods for effective process optimization solutions. The principle of dynamic programming is to evaluate the smallest subproblems until the largest. The algorithm based on the principle of dynamic programming is described in 4 points [19]:

- creating characteristics of the optimal solution,
- defining a recursive optimal solution,
- solving the task from the smallest problems,
- constructing a solution from calculations.

In the case of the shortest path, we will use the theory of graphs and networks, and therefore it is necessary to introduce the terminology used. The first and main term is an acyclic network, which can be represented by a graph having a nonempty finite set of nodes $V = \{v_i\}$ and a set of edges $H = \{h_{i,j}\}$. The acyclic network can be described by a subset $V \times V$, which determines the topology of the graph.

The elements of the set $h_{i,j} = \{v_i, v_j\}$ are thus the edges of the network, which express the existence of the transition from node v_i to node v_j . A node from which at least two edges protrude is called a branching node. The result we need to get from the solution is a path or route $S \{v_1, v_2, \dots, v_n\}$ with a finite sequence corresponding to the node for the shortest path [4].

In our case, it will be an acyclic network with 20 points, which is shown in (Fig.3). Nodes are represented by an empty circle in which the own sequence number is given. The edges represent the lines that connect the nodes, and the numbers above the edges are the distance between the nodes. The symbol C_i denotes the distance to the target point.

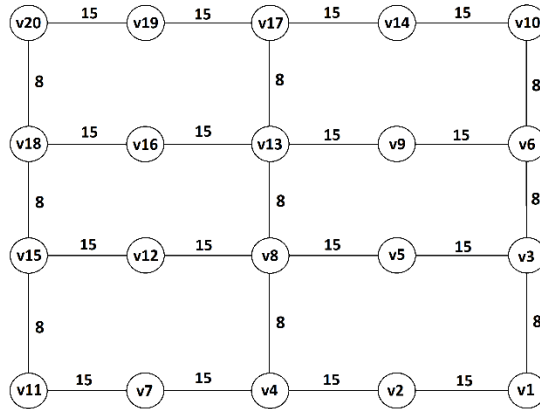


Fig.3. Acyclic network of application.

We will clearly explain the whole principle on the example with the start node v_1 and the end node v_9 in three steps. In the first step, starting from node v_1 , whose adjacent nodes are v_2 with a distance to the end point of 46 meters and v_3 of 23 meters, we find that the node v_3 is closer to the end node and we move to it (Fig.4a). In the second step, we have a choice of three adjacent nodes v_1 , v_5 and v_6 , again we compare their distances to the end point and move to the nearest, which corresponds to node v_6 (Fig.4b). In the third step, the source node v_6 also has three adjacent nodes v_3 , v_9 and v_{10} . It can be seen (Fig.4c) that the node v_9 has a distance of 0, as it is the end point. We move to it and find the shortest route between nodes v_1 and v_9 .

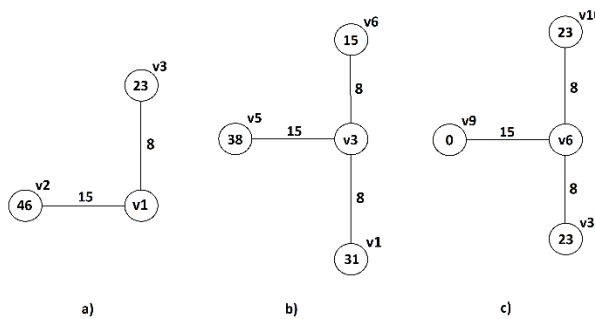


Fig.4. The procedure for finding the shortest path.

c) Application Design

The application is created in Promotic environment, version 8.3.11, using a developer license. The license allows the use of an unlimited number of variables (329 variables were used in the work) with a limited runtime for one hour. The application consists of HMI and the structure of global objects. The structure of objects is divided according to their type. A separate folder with a corresponding name is created for each object type. We also tried to name each object authentically according to its function for better consistency of application scripts.



Fig.5. The main panel: Roofs, Colors, Insulation, Flooring, Cement, Pavement.

In the following section, we will describe all the objects that make up HMI applications and we will take a closer look at all the elements in the panel and their functionality. As mentioned above, the main panel is the warehouse panel, which is displayed to the user after entering the login details correctly. Therefore, we will clarify this panel first.

The main panel consists of two parts, the control panel and the display panel. The display panel provides a top view of the warehouse with information about the category of shelves and to display the filling of the warehouse after selecting a certain side of the shelf, it opens a modal rack window, the functionality of which we will explain in the next section. It also provides a display of the shortest route when instructed by the storekeeper. The control panel, in turn, provides a change in the color of the environment, the display of the legend, the display of the next or previous route, the logout of the user and the loading or unloading of goods from the shelf. We will describe all these functionalities in more detail below.

The application contains three modal windows, which can be accessed from the main window. These modal windows are the main functions of the application. Next, we will describe all modal windows found in the application.

The modal import window shows us the environment in which the user can insert the parameters of the package and then write them to the database. The main parameters are the six-digit number of the package in the range from 000001 - 999999, the category to which the package belongs, its weight in kilograms, the number of pieces and the name of the goods. The application is created for packages on euro pallets, so the X and Y dimensions are predefined to the dimensions of the euro pallet in centimeters.

The modal export window allows you to search for packages in the database after entering the name in the Product field and the number of pieces in the Number of pieces field. After entering the values and pressing the Load button, the package corresponding to the number of pieces will be searched, or several packages, if the selected number of pieces is not contained in one package. If there are not enough pieces of the selected product in the database, the text will appear in the notification window: “There are not enough pieces of goods in stock!”.

Alternatively, if there is no package with the specified name in the warehouse, the notification window will display: “The given goods are not in the warehouse!”. However, if a package with a sufficient number of pieces is in the database, a notification window will display the message: “Package found” and a table drawn by the Canvas method in JavaScript will be displayed with the number and storage of the found package.

The image shows two side-by-side screenshots of application windows. The left window, titled 'Vyskladnenie', displays a 'Produkt' field with 'CRH 25I' and a 'Počet kusov' field with '50'. Below this is a table with columns 'Číslo balíka', 'Regál', 'Strana', and 'Segment'. The table contains three rows of data. At the bottom, there is a green bar with the text 'Balík sa našiel' and a 'Načítať' button.

| Číslo balíka | Regál | Strana | Segment |
|--------------|-------|--------|---------|
| 52 | 5 | 2 | 200 |
| 53 | 5 | 2 | 199 |
| 54 | 5 | 2 | 198 |

The right window, titled 'Naskladnenie', displays a 'Číslo balíka' field with '000052', an 'Hmotnosť' field with '1000', and a 'Počet kusov' field with '20'. It also has a 'Názov tovaru' field with 'CRH 25I'. On the right side, there is a 'Kategória' section with radio buttons for 'Strechy', 'Farby', 'Izolácia', 'Podlahy', 'Cement', and 'Dlažby'. Below this is a table for dimensions with columns 'X', 'Rožmery', and 'Y', showing values '120' and '200'. At the bottom, there is an 'Oznam' field and a 'Zápis' button.

Fig.6. The modal Export Window (left): **Stock-out**, 50 pieces, Number of package, Numbers of position, green text: Package is found, Read button.
The modal Import Window (right): **Stock-in**, Package number weight pieces, Name of item, Category, Dimensions XY, Write button.

The modal rack window displays all full segments on a given side of the rack with the name of the package that is in the segment. This allows the user to see which packages are physically in stock. There is also a Back button in this modal window that allows you to close the modal window.

The screenshot shows a grid of chemical packages. The top row contains 'Weber penetrácia 0,5L' and two 'Dulux zelená' packages. The middle row contains two 'Hetmat Plus 1L' packages and two 'Dulux biela' packages. The bottom row contains two 'Hetmat Klasik 1,5L' packages and two 'Dulux čierna' packages. A 'Späť' button is located at the bottom right.

Fig.7. The modal rack window: names and flask volumes of chemicals in stock.

Finding the shortest path consists of three main steps. In the first step of inserting and unloading packages from the warehouse, according to the entered data, suitable storages will be found, which will be written to a text file in a common directory for both applications. In this way, all entered data is written with the found segments into which packages can be inserted or taken. This process is repeated until the modal import or export window is closed. This will allow the application to decide on the optimal sequence of the warehouse keeper’s interaction with the packages on the road.

The second step is to get the values of the distance from the current point where we are to the given segment from the Distance table for each segment from the text file. For each segment, we compare its distance value with previous values of segments that have already been compared. If the value of the segment being compared is less than the previous one, its distance value is entered in the variable Shortest Distance and in the appropriate field the number of the rack and the number of the page in which the segment is located. After comparing all the segments from the text file, we delete the package, which we insert first into the warehouse and all its suitable segments. This will get the package with the next save and perform the third step for the obtained save.

In the third step, we will use the knowledge of dynamic programming, while we have the current node in which we are and the node in which we need to get. First, we read the values from the database of dynamic programming values, specifically from the neighbor table for the current point. This will get all the nodes connected to the current point and for each of them we will get the value of the distance to the end node. Evaluate the node that has the shortest distance to the end node as the current node and set the visibility of the respective edge to true in the visibility field. We perform this procedure until the current point is the end point. When we arrive at the end node, we load all suitable segments on the given side of the rack, select the nearest segment and set the end node as the current one. The visibility field is then written to a text file, from which the paths to the packages are later read. When specifying multiple packages for picking or stocking, steps two and three are repeated for all packages entered.

The application also contains additional functions for better work with the application, increased security of the application and faster acquaintance of the user with the application. Next, we exchange and describe all additional functions that the application contains.

As with all systems, our application requires credentials to run. The registration is performed by the administrator, as the application is intended for a narrow working team. Login is not case sensitive. After pressing the Login button, the entered data are compared with the data from the database and, if they match, the main panel is opened. When logging in, the user can choose one of the seven languages in which the application interface will be displayed. The default language is Slovak, after pressing one of the buttons in the language selection section, the texts will be overwritten in the selected language and the value of the selected language will be entered into the database. This outlines another function of the application, where after logging in, the language of the application changes to the last language selected by the user.



Fig.8. Login+Password+Language panel (left), Help panel (right): shelf number 1-6.

Another feature of the application is help. Help provides information about all the elements that are on the taskbar. When the help is activated, all buttons are highlighted in pale blue and the information panel is displayed at the top of the window. When you press one of the buttons, its function appears in the information bar.

The application includes the ability to switch between day and night mode. The difference between these two modes is the color of the application interface. In day mode, the elements are brighter with black text to achieve optimal visibility in daylight. In night mode, the elements darken, the background is highlighted, and the text turns white. This maintains the same visibility of the elements, but with less contrast of the colors of the elements at night. Mode switching is set to automatic switching when the application is opened, day mode is active from 6:00 to 18:00 and night mode at night from 18:00. The user can also choose to turn off automatic switching and set the mode manually.

Conclusion

The aim of the paper was to develop and to create an application with optimization of material movement in the warehouse. We dealt with the calculation and subsequent display of the shortest path to the packages that needed to be stored in or removed from storage.

The developed application could be used in warehouses of various sizes and employee structures. The application would run separately on multiple devices, connecting to a database stored in the cloud that would be common to all devices.

Two situations can occur in a company. The first one is that one employee would be in charge of recording the packages received in the warehouse or removed from storage to hand over the packages from the warehouse. The second employee would be shown the shortest way to remove or store packages. The second situation is that one employee performs both options, in this case he would enter the packages into the application himself, to which he would then see the shortest route.

Acknowledgement

This paper was supported by the Scientific Grant APVV-17-0190 and by Scientific Grants the Slovak Grant Agency KEGA 016STU-4/2020 and 039STU-4/2021.

References

- [1] Poatsy M. A., Williams J., Rutledge A. (2019), *Exploring Microsoft Office Access 2019 Comprehensive Spiral-bound*, ISBN 978-01-354-3581-6
- [2] Koreň, M. (2009). *Databázové systémy*, ISBN 978-80-228-2084-4
- [3] Delikát, Tomáš; *Základy databázových systémov*. 2006. ISBN 809694844X
- [4] Hudzovič, Peter: *Optimalizácia*. 2001. ISBN 85-259-2001
- [5] Poorvika Prakash (2019), *Pick to Light, Light-directed picking technology in Warehouse | Adverb*, <https://medium.com/@prakashpoorvika/pick-to-light-voice-picking-technology-in-warehouse-adverb-59eba48a8cde>
- [6] Promotic, *Přehled Web technologie v systému PROMOTIC*, <https://www.promotic.eu/cz/pmdoc/Subsystems/Web/Web.htm>
- [7] SvetDopravy. *Systémy skladovania v logistických centrách*, <http://www.svetdopravy.sk/systemy-skladovania-v-logistickych-centrach/>

- [8] Transport Geography. Cross-Docking Distribution Center, https://transportgeography.org/?page_id=4453
- [9] LightningPick. Pick-to-Light, <https://lightningpick.com/products/pick-to-light/>
- [10] PuttoLight. Put-to-light Overview, <https://puttolight.com/overview/>
- [11] W3school. DBMS Introduction, <https://www.w3schools.in/dbms/intro/>
- [12] Worldvector. Microsoft Access 2013 logo, <https://worldvectorlogo.com/logo/microsoft-access-2013>
- [13] Oshiro. Scada - SCADA Remote Terminal Unit Modbus Programmable Logic Controllers Diagram, https://favpng.com/png_view/scada-scada-remote-terminal-unit-modbus-programmable-logic-controllers-diagram-png/SkP7eHt1
- [14] Tutorialspoint. MS ACCESS – Overview, https://www.tutorialspoint.com/ms_access/ms_access_overview.htm
- [15] SCADA Systems. SCADA systems, <http://www.scadasystems.net/>
- [16] Ing. Ján Cigánek PhD., Database and visualization systems – lectures.
- [17] Promotic. Co je Promotic, <https://www.promotic.eu/cz/pmdoc/WhatIsPromotic/WhatIsPromotic.htm>
- [18] Promotic. Databázové možnosti v systéme Promotic, <https://www.promotic.eu/cz/pmdoc/Subsystems/Db/Database.htm>
- [19] Input. Dynamické programovanie, <http://input.sk/struct2017/08.html>

▲ Authors



Ing. Filip Žemla

Faculty of Electrical Engineering and Information Technology,
Slovak University of Technology in Bratislava, Slovakia
filip.zemla@icloud.com

Currently a student of doctoral studies at Slovak University of Technology in Bratislava. The main focus of his studies is oriented to virtualization and optimisation of modern manufacture processes. His main skills are SCADA systems, database systems and front-end programming.



Ing. Ján Cigánek, PhD.

Faculty of Electrical Engineering and Information Technology,
Slovak University of Technology in Bratislava, Slovakia
jan.ciganek@stuba.sk

He was born in 1981 in Malacky, Slovakia. He received the diploma and PhD. degree in Automatic Control from the Faculty of Electrical Engineering and Information Technology, Slovak University of Technology (FEI STU) in Bratislava, in 2005 and 2010, respectively. He is now Assistant Professor at Institute of Automotive Mechatronics FEI STU in Bratislava. His research interests include optimization, robust control design, computational tools, SCADA systems, big data, and hybrid systems.

PROBLEMS OF DATA TRANSFER IN THE NETWORK OF THE ORGANIZATION WITH MINIMIZED CAPABILITIES OF THE USED RESOURCES

Andrey Preobrazhenski, Igor Lvovich, Yury Preobrazhenski

Abstract:

Currently, communication networks are actively developed and evolve, which requires connection of many stations now. Among them are quite a few networks that use LTE technology. It was necessary to create a mathematical model that allows to serve a different type of traffic in LTE networks, as well as implement it. Using this model, it was necessary to evaluate how well applications are served, and then build a system that allows to describe the characteristics of its work, using the results to create a list of recommended actions when managing traffic of various types in real time. The results are given on the assessment of the rate with which the transfer takes place in the part of the LTE-network, in which it is possible to process applications for all types of traffic, with a limited value of losses. Results are shown on estimation of rate value in cell, which will allow processing of requests for all types of traffic, with permissible losses and averaged time for data transmission. The average use of cell resources in data transmission is demonstrated, in the case where resources are maximally available to transmit data traffic.

Keywords:

Computer network, traffic loading, protocol.

ACM Computing Classification System:

Network protocols, network algorithms, network types.

■ Introduction

The use of 4th generation mobile networks, which are based on technological solutions that allow access from many stations, and have orthogonal OFDMA modulation, using MIMO encoding, allows traffic to be transmitted in greater volume than in previous generation of networks.

These networks are characterized by a very flexible architecture, they can change network topology when connecting, disconnecting users. In addition, they had high data rates that need to be reliably protected from hacking. These networks did not use expensive cabling, which made them cheaper to access.

LTE networks are controlled by base stations. They, together with the main network survey, can determine the routes on which traffic from clients will be directed. But here the main difficulty is to manage it on the interface with compliance with quality requirements (QoS), considering all subscriber services, for example, roaming.

Since mobile applications had recently grown significantly in quantity, that required a high quality of service that could be achieved if the radio interface had a high throughput capacity. Because when using wireless access, load differences are possible due to the fact that users move in stochastic order [1].

As mobile communication becomes cheaper, new types of client-terminals arise, and services that addressably transmit video data develop, then real-time traffic increases accordingly. And its speed indicators must be unchanged.

The purpose of the paper is to develop and describe a model, implement an algorithm for increasing the capacity of the radio interface in LTE networks.

This algorithm is based on the use of a minimum amount of resources per month to analyze different service models, which is achieved by effectively controlling the rate at the time of data transmission.

1 Modeling of Application Distribution in LTE Network

Let's look at the development of algorithmic solutions that will allow you to regulate access to new applications on the network. A simulation model was created that allows to evaluate the traffic of various kinds coming to part of the LTE network. Consider a mathematical model for processing traffic having two real-time rates relative to a portion of the LTE network [2].

To process a single request, you must provide one hundredth of resources c_r bit/second. The real-time application processing time indicator r is distributed exponentially according to the average indicator $1/\mu_r$. In this case, μ_r is a parameter describing this distribution.

In addition, we indicate that applications for the transfer of files will be received in accordance with the Poisson law, at intensity - λ_d . To process a single request, the cell is given the maximum available amount of resources, with a size of c_d bit/second, which corresponds to an expression $c_1 \leq c_d \leq c_2$. The values c_1 , as well as c_2 , determine the minimum and maximum speed at which files will be downloaded. Take that $c_1 \leq c_2$.

The model in question determines that the file to be transmitted will be exponentially determined having an average of F (bit). It was clear that the value of time to transfer a file, using exclusively c_1 (minimum speed) and c_2 (maximum speed), would be distributed exponentially, with parameters $\mu_{d,1}$ and $\mu_{d,2}$. Parameters $\mu_{d,1}$ and $\mu_{d,2}$ are found using an expression $\mu_{d,1} = c_1/F$ and $\mu_{d,2} = c_2/F$.

2 Results of Transmission Rate Estimation on LTE Cell Fragment

The characteristics of the model load will be the intensity of traffic in real time λ_r , as well as the intensity of data traffic λ_d .

The main parameter that will determine and allocate resources over the data transfer will be speed. It was clear that if one were to sort, it was possible to estimate each parameter presented if the others were fixed. It was recommended that those applications submitted in real time should be considered a function that would evaluate the quality parameter when processing incoming applications πr that they had not received access.

Clearly, if you browse, it is possible to evaluate each parameter presented if others are fixed AND applications transmitting πd files that also do not have access. By planning data transmission resources, these indicators can change. Further, when conducting the study, we will take this fact into account.

Let us assume that the main value of lost bids will be π , the value of which can be determined using some expression. It was recommended that those applications submitted in real time should be considered a function that would evaluate the quality parameter when processing incoming applications πr that they had not received access.

$$\pi = \max(\pi_r, \pi_d)$$

As another equally important parameter that evaluates the quality of file transfer request processing, we will select the average time required to transfer the file T_d . We estimate the transfer resource which has a cell acceptable to handle incoming traffic flows according to the required quality. The quality parameter in the processing of requisitions is determined by the fact that $\pi = 0,05$. if subsequent model parameters are calculated:

$$C = 100 \frac{Mbit}{s}, c_r = 3 \frac{Mbit}{s}, c_1 = 1 \frac{Mbit}{s}, c_2 = 5 \frac{Mbit}{s}, F = 16 Mbit, \mu_e = \frac{1}{300}, \lambda_r = 0,05, \lambda_d = 5.$$

If there are such values, the loss will be defined as $\pi_r = 0,3274, \pi_d = 0,1299$. And any parameter value will be greater than π on 0,05.

Next, we will systematically increase the rate at which the data are transmitted until the maximum loss is at least 0.05.

The results of the calculations are shown in (Fig.1).

It presents the results of calculated losses on applications πr , as well as πd , if the data transfer rate increases C. Of course, if the speed C increases, then the loss rate on applications decreases.

From $C = 118 \frac{Mbit}{s}$, the amount of losses on requests for data transfer will be less than 0.05, and from $C = 129 \frac{Mbit}{s}$, real-time traffic processing requests will also lose less than 0.05. Accordingly, the problem is solved with the value $C = 129 \frac{Mbit}{s}$.

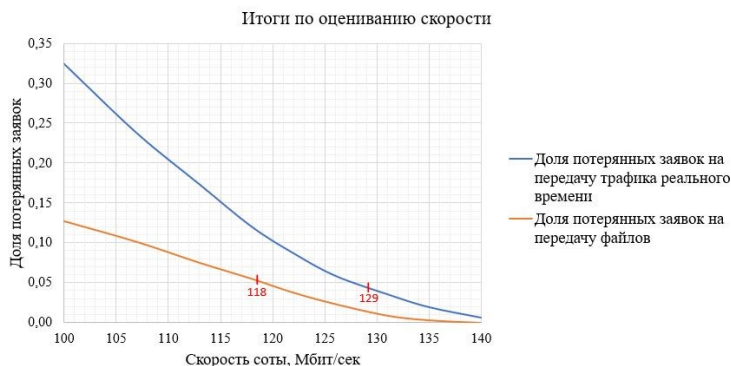


Fig.1. Results on estimation of the rate at which the transmission takes place in the part of the LTE network at which requests for all types of traffic can be processed, with the limit loss value.

Horizontal axis: velocity Mbit/sec,
 upper blue line: real time loss rate of requests,
 lower yellow line: file transfer loss rate of requests.

To find a transfer resource, its volume, often it is required to calculate average time necessary to transfer the file and which will be sufficient to process traffic according to quality parameters.

Suppose the model requires an average transmission time of T_d of not more than five seconds [3].

In this case, the transfer resource is selected until the corresponding condition is fulfilled and the corresponding time parameter is fulfilled with it. The results of this task are shown in (Fig.2).

It shows the average time to transfer file T_d with the condition of increasing the total data rate C .

Naturally, when C is increased, the value of the file T_d will decrease. From the indicator $C = 137 \frac{Mbit}{s}$, the value of losses on applications for all types of traffic will be less than 0.05, while the average time to transfer a file will be less than five seconds. And the task was solved with $C = 137 \frac{Mbit}{s}$.

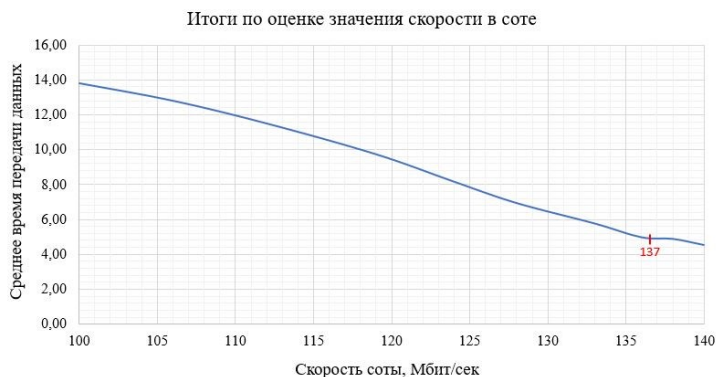


Fig.2. Estimates of the rate in the cell, which will allow the processing of requests for all types of traffic, with permissible losses and average transmission time.

Horizontal axis: velocity Mbit/sec,
vertical axis: average time of data transfer.

Also, the maximum allowed amount of traffic passing through the cell with constant capacity to pass C is selected, as well as with the value of maximum additional losses. As a normative indicator, the average time limit for data transmission is also applied.

To achieve this, if other parameters are constant, the resource load in the cell will decrease until the quality restrictions of the incoming requests are fulfilled [4].

The results of the calculations are shown in (Fig.3). Real-time bid losses are calculated here π_k , as well as for file transfer requests π_e , with reduced load ρ . Of course with a decrease ρ reduced number of losses on applications. If ρ will be less than 0,95, then the amount of losses on applications for all types of traffic will be less than 0.05.

The problem was solved with a value of then the amount of losses on applications for all types of traffic will be less than 0.05.

The problem was solved with a value of $\rho = 0,95$. Value size λ_r , and also λ_d . The size of the values is determined by the relation that finds about ρ . To solve this problem, you need to know how the intensities for all types of traffic that we analyze relate to each other [5].

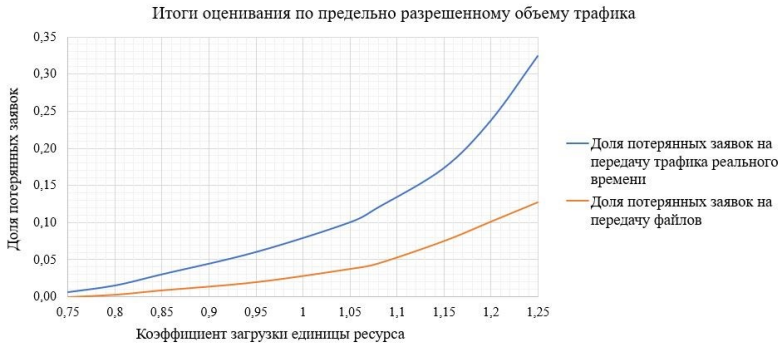


Fig.3. Results of estimation by the maximum allowed traffic volume that passes through the cell, with constant data throughput C , as well as with specified marginal losses. Horizontal axis: load ratio of cell unit, vertical axis: loss rate of requests, upper blue line: real time loss rate, lower yellow line: file transfer loss rate.

3 Investigation of the Algorithm for Selecting the Ratio between the Minimum and Maximum File Transfer Rates

Let's go on to consider the problem of choosing the ratios of mines c_1 , and also max c_2 data rates. Of course, what if $c_1 = c_2$, then file processing will take place using the Erlang model. If the speed value c_2 . increases, then the network operator accelerates the data transmission. To do this, the capacity of the cell itself is used, which is free and does not process traffic in real time.

Let's show this process by example. Imagine a cell with numerical parameters such as:

$$C = 100 \frac{Mbit}{s}, c_r = 3 \frac{Mbit}{s}, c_1 = 1 \frac{Mbit}{s},$$

$$c_2 = 1 \frac{Mbit}{s}, F = 16 Mbit, \mu_r = \frac{1}{300}, \lambda_r = 0,04, \lambda_d = 4 call / s.$$

We have already said that if you select these entry parameters, then the processing of applications will be presented using the Erlang model. And with an increase c_2 with constant other parameters, the capacity in the cell will be better since the data will be transmitted at a higher rate.

Let's take this as an example.

The results of the calculations are shown in (Fig.4). It shows real-time loss calculation π_r , and when transmitting information π_d with an increase of the indicator c_2 one to forty Mbps.

Of course, with an increase in the indicator c_2 there is a decrease in losses on applications. This process will be the same for all traffic requests. The occurrence of such dependence occurs since resources are released in an accelerated manner. If the conditions described above were accepted, the greatest efficiency would be achieved if $c_2 = 10\text{Mbit} / \text{s}$.

Subsequent promotion c_2 does not have much influence on characteristics [6, 7].

Given this, we can say that the interval for changing the speed value with which files are transmitted is selected from how the parameters relate to each other. And this choice can be made by using a built-in model, together with algorithms that can evaluate its characteristics.



Fig.4. Dependencies of losses by claims, if resource transmitting traffic is as accessible as possible π_f , if speed rises c_2 . Naturally, when the speed increases c_2 , the load in the cell will also increase. Horizontal axis: upper limit of file transfer velocity, vertical axis: loss rate of requests, upper blue line: real time loss rate, lower yellow line: file transfer loss rate.

(Fig.6) presents the results of calculations of the average number of applications for any of the category m_r as well as m_d , which contains the cell in processing if the index rises c_2 .

You can see that when zoomed in c_2 , the average number of file transfer requests that are accepted for processing will decrease. Due to the fact that these applications are processed faster by the system and leave it.

(Fig.7) presents the results of the calculations of the averages for the distribution of cost-effectiveness and s_d directly in part of the network. As well as their total values, which are used for all types of traffic. If increases c_2 , the use of resources will change only initially, after these changes will not be significant.

(Fig.8) is a summary of calculations of the average utilization of cell c_d resources in file transfer. When c_2 is increased, this parameter will also be increased, but it is the initial operation.

(Fig.9) is a summary of the average time calculations for file transfer T_d if increases c_2 . is raised from one to forty one Mbps. By increasing c_2 , the average data transmission time will decrease from a value of sixteen seconds and will decrease to a value of 6.2 seconds, depending on how the cell is loaded.



Fig.5. Results of calculations of part of time at whole load of cell resources, in case, when resource availability increases when transferring file traffic. Horizontal axis: upper limit of data transfer velocity, vertical axis: time rate.

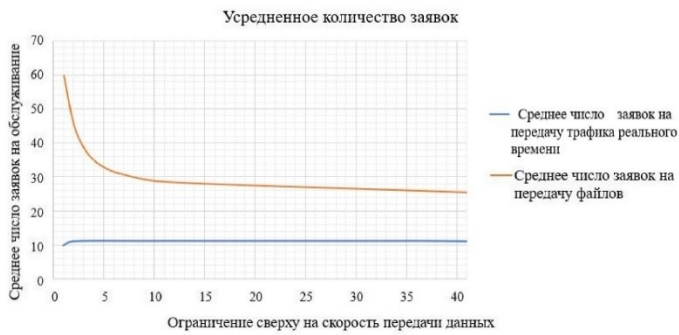


Fig.6. The average number of requests that a cell contains in processing, in the case where resources are maximally available when transmitting information traffic. Horizontal axis: upper limit of data transfer velocity, vertical axis: average number of requests.

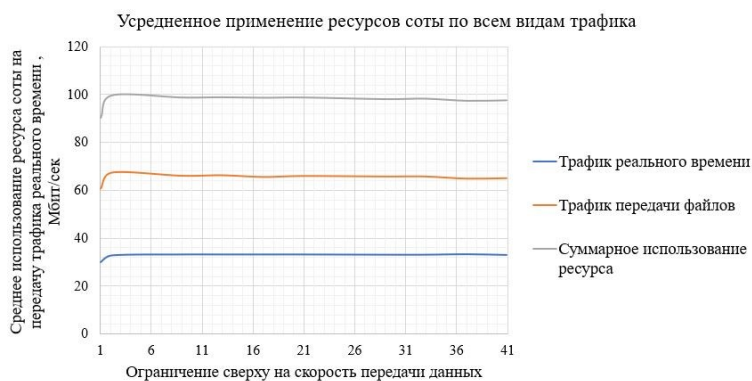


Fig.7. Average utilization of cell resources across all types of traffic, in the case where resources are maximally available to transmit data traffic. Horizontal axis: upper limit of data transfer velocity, vertical axis: average utilisation Mbit/sec.

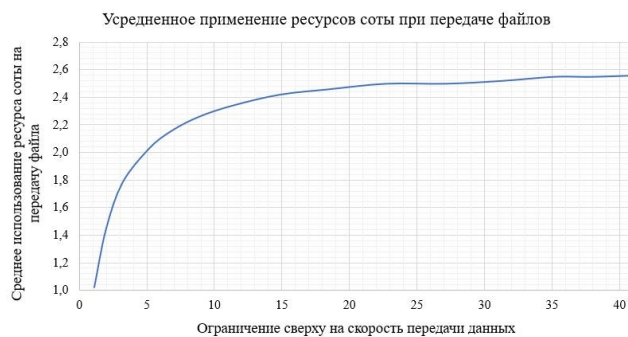


Fig.8. Average use of cell resources in file transfers when resources are as available as possible to transmit data traffic. Horizontal axis: upper limit of data transfer velocity.



Fig.9. Average use of cell resources in data transmission, in case when maximum resources are available for data traffic.

Horizontal axis: upper limit of data transfer velocity, vertical axis: average time of data transfer.

Conclusion

There was introduced an algorithm to solve the problems of planning the way to skip the data of a part of the network. In addition, the maximum amount of traffic allowed was determined, with its transmission in accordance with the established quality requirements. It is determined how restrictions are related to the rate at which files are transferred in order to increase the efficiency of using the resources of a part of the network.

References

- [1] Panevin R., Yu., Preobrazhensky Yu., P. (2008) Structural and functional requirements for a software package for presenting knowledge. *Bulletin of the Voronezh Institute of High Technologies*. No. 3. S. 061-064.
- [2] Preobrazhensky Yu., P., Marenkov N., M. (2020) Analysis of algorithms useful in the formation of augmented reality systems. *Bulletin of the Voronezh Institute of High Technologies*. *Bulletin of the Voronezh Institute of High Technologies*. No. 1. S. 40-42.
- [3] Preobrazhensky Yu., P., Myasnikov N., M. (2020) Analysis of the prospects of information technology in the field of Internet of Things. *Bulletin of the Voronezh Institute of High Technologies*. No. 1. S. 43-45.
- [4] Pustynnik I., E., Preobrazhensky Yu., P. (2019) Securing messages between the server and IoT devices. *Bulletin of the Voronezh Institute of High Technologies*. *Bulletin of the Voronezh Institute of High Technologies*. No. 4. S. 40-45.
- [5] Lvovich I., Ya., Preobrazhenskiy A., P., Preobrazhensky Yu., P., Choporov O., N. (2019) About tracking processes on various devices. *Bulletin of the Voronezh Institute of High Technologies*. No. 4. S. 49-51.
- [6] Lvovich I., Ya., Preobrazhenskiy A., P., Preobrazhensky Yu., P., Choporov O., N. (2019) On the quality of the Internet of Things system. *Bulletin of the Voronezh Institute of High Technologies*. No. 9. S. 52-55.
- [7] Preobrazhensky Yu., P., Miroshnik D., N. (2018) Analysis of fuzzy search methods. *Bulletin of the Voronezh Institute of High Technologies*. No. 4. S. 82-84.

▲ Authors



Prof. Andrey Preobrazhenski

Doctor of Sciences (Engineering), Professor,
Voronezh Institute of High Technologies, Voronezh, Russia
E-mail: app@vivtl.ru



Prof. Igor Lvovich

Doctor of Sciences (Engineering), Professor,
Voronezh Institute of High Technologies, Voronezh, Russia
E-mail: office@vivt.ru



Prof. Yury Preobrazhenski

Candidate of Sciences (Engineering), Professor
Voronezh State Technical University, Voronezh, Russia
E-mail: petrovich@vivt.ru

COMPARISON AND ANALYSIS OF THE USE OF ADVANCED METHODS OF ARTIFICIAL INTELLIGENCE FOR NEURODEGENERATIVE DISEASES

Eugen Ružický, Štefan Kozák, Ján Lacko, Juraj Štefanovič,
Alfréd Zimmermann, Milan Rusko, Petra Brandoburová, Matej Škorvánek

Abstract:

The paper deals with the comparison of existing methods of using artificial intelligence (AI) for the effective diagnosis of selected neurodegenerative diseases. The use of AI for disease diagnosis has advanced significantly in the last decade, as well as the use of various machine learning methods of speech recognition for disease diagnosis. The use of new technologies based on AI can help find a solution to a non-invasive, easy-to-apply method for detection and subsequent treatment of brain diseases. Diagnosis of neurodegenerative diseases has mainly been performed using neuroimaging methods such as magnetic resonance imaging or positron emission tomography or single-photon emission computed tomography. The aim was to analyse existing AI-assisted diagnostic approaches based on peer-reviewed publications and to highlight current trends in the diagnosis of Alzheimer's and Parkinson's diseases. Finally, we showed our approach to early diagnosis of neurodegenerative diseases.

Keywords:

Neurodegenerative diseases, Alzheimer's disease, Parkinson's disease, spontaneous speech, artificial intelligence, machine learning, deep learning.

ACM Computing Classification System:

Machine learning algorithms, machine translation, natural language generation, speech recognition, lexical semantics, phonology.

▀ **Introduction**

The most common neurodegenerative diseases are Alzheimer's disease (AD), Parkinson's disease (PD) and others, which are often determined by neurological and psychiatric examination using a variety of ancillary tests such as magnetic resonance imaging (MRI), positron emission tomography (PET), speech and vision tests or laboratory tests of cerebrospinal fluid (CSF) or blood. In this article, we focus on two neurodegenerative diseases in particular: AD, including the Mild Cognitive Impairment stage (MCI), and PD.

Around 35 million people worldwide live with AD or another dementia. By 2030, the number is expected to exceed 65 million. Alzheimer's disease and other forms of dementia are currently among the 10 most common causes of death worldwide, with the 3rd most common deaths in Europe and the United States in 2019 [1].

The number of patients with neurodegenerative diseases in the world is increasing every year, similarly in Slovakia, according to the data of the National Centre of Health Information in Slovakia there are more than 40 thousand of them and according to the latest surveys it is up to twice as many [2].

1 Current Research on Neurodegenerative Diseases

The goal of our Early Warning of Alzheimer's (EWA) project is to develop a data collection methodology, select appropriate images, videos, questions and procedures to collect input data for early diagnosis of AD, MCI and PD, especially using speech recognition. As part of the EWA project, we analysed publications on neurodegenerative diseases and developed a research review until 2020. Authors Boschi and colleagues analysed the speech of people with neurodegenerative diseases [3]. They performed a systematic analysis of 61 publications focusing on language variables extracted from patients' speech up to 2017. In their analysis of spontaneous speech, they investigated the phonetic, phonological, lexical-semantic, morphosyntactic and pragmatic levels of language, for which they defined different characteristic linguistic variables. Their conclusions are as follows: Alzheimer's disease is most pronounced at the lexico-semantic (80%), discourse-pragmatic (77%), syntactic (57%) and phonetic (55%) levels. In patients' speech, it manifests itself at the semantic level by word finding, word correction and repetition [4]. At the phonetic level, the speech of AD patients is mainly characterized by low frequency of speech and frequent hesitations [5]. When comparing amnesic mild cognitive impairment (aMCI) and AD, aMCI patients were found to use a greater number of correct nouns instead of pronouns than Alzheimer's patients. Similarly, aMCI patients' interviews appear to be more effective, coherent, and informative than Alzheimer's patients' interviews.

Parkinson's disease (PD) is often associated with motor speech impairment that affects phonation, articulation, resonance, and prosody [6], detected mainly by variables related to pause duration [7] and change in prosody [8]. Language deficits include morpho-syntactic processing, especially verb generation [9]. An important summary of the results for AD, aMCI and PD is shown in Table 1, Table 2 and Table 3 adapted from [3], where aMCI is the amnesic MCI and abbreviation SD means standard deviation.

Table 1. Relevant linguistic features for AD, aMCI and PD versus Healthy Controls (HC).

| Linguistic level | Linguistic feature | AD vs. HC | aMCI vs. HC | PD vs. HC |
|------------------|----------------------------------|-----------|-------------|-----------|
| Phonetic and | Speech rate | AD < HC | - | not rel. |
| Phonological | Number of pauses | - | - | PD > HC |
| | Between-utterance pause duration | - | - | PD > HC |
| | Prosody: F0 SD | not rel. | - | PD < HC |
| | Prosody: Intensity SD | - | - | PD < HC |
| | Hesitation ratio | AD > HC | - | - |
| Lexicosemantic | Pronoun-noun ratio | AD > HC | - | - |
| | Closed-class words | AD > HC | not rel. | not rel. |
| | Idea density | AD < HC | - | - |
| | Frequency | AD > HC | - | - |
| | Semantic errors | AD > HC | - | - |
| | Word-finding difficulties | AD > HC | - | - |
| | Indefinite terms | AD > HC | - | - |

Table 2. Relevant linguistic features for AD versus HC and for PD versus HC.

| Linguistic level | Linguistic feature | AD vs. HC | PD vs. HC |
|------------------|---------------------------|-----------|-----------|
| Morphosyntactic | Inflectional errors | AD > HC | not rel. |
| Syntactic | Mean length of utterances | AD < HC | not rel. |
| | Reduced sentences | AD > HC | - |
| Discourse | Discourse markers | AD > HC | - |
| and | Cohesion | AD < HC | - |
| Pragmatic | Correct pronoun | AD < HC | - |
| | Local coherence | AD < HC | not rel. |
| | Global coherence | AD < HC | not rel. |

Table 3. Comparison between Alzheimer’s disease and amnesic Mild Cognitive Impairment.

| Linguistic level | Linguistic feature | AD vs. aMCI |
|--------------------------|----------------------------------|-------------|
| Lexico-semantic features | Pronoun rate | AD > aMCI |
| | Idea density | AD < aMCI |
| Discourse and pragmatic | Information content | AD < aMCI |
| features | Index of discourse effectiveness | AD < aMCI |
| | Efficiency | AD < aMCI |

2 Alzheimer's Disease

We searched the SCOPUS database for review publications for Alzheimer's disease [10], [11]. Until 1984, the diagnosis of patients with AD was almost entirely based on clinical examination [10], mainly using the Mini Mental State Examination (MMSE) or the Montreal Cognitive Assessment (MoCA). At present, magnetic resonance imaging (MRI) and positron emission tomography (PET) have led to a broader understanding of neuropathological processes. In addition to expensive neuroimaging and detailed medical examination, there is an invasive analysis of cerebrospinal fluid (CSF) [12]. However, cheaper other approaches are being sought, such as blood biomarkers and spontaneous speech analysis using artificial intelligence. No blood biomarker has yet achieved sufficient accuracy [13].

In the analysis of spontaneous speech, prosody is most often studied in people with neurodegenerative diseases because it relates to the phonetic and phonological properties of speech. Specifically, it involves the analysis of speech rhythm along with other parameters related to temporal and acoustic measures of voice, such as articulatory rhythm, vocal intensity (analysis of loudness and changes in amplitude over time), timing and frequency (changes in acoustic signal frequencies, colour or shape structure). There are several studies that jointly evaluate the process of extracting features from the vocal signal using different vocal parameters and different qualifiers [10].

For the analysis of spontaneous speech and sound, the following Table 4 lists the common properties used to describe the acoustic characteristics of the voice used to detect AD [11]. We use abbreviation F0: Fundamental Frequency, SD: Standard Deviation, VR: Variation Range.

Table 4. Main conventional features used in Alzheimer's disease.

| | | |
|----------------------------|------------------------------------|--|
| Phonetic aspects | Interruptions | Percentage and number of pauses of voice, Percentage without voice |
| | | Number and percentage of voice breaks |
| | | (MEAN, MAX, MIN) |
| | Voice periods | Number of pulses analysed as voice |
| Period (MEAN, SD) | | |
| Frequential Aspects | Fundamental frequency and spectrum | F0 (MEAN, MAX, MIN, SD, VR) |
| | | Short time energy or spectral centroid |
| | | High and low global pitch |
| | | Autocorrelation |
| | Fluctuations | Jitter (Short term, cycle-to-cycle, perturbations in the F0): local jitter, local absolute jitter, relative average perturbation jitter |
| Intensity | Amplitude | Intensity of voice and unvoiced signals (SD, MAX, MIN) |
| | | Square Energy Operator (SD) |
| | | Teager-Kaiser Energy Operator (SD) |
| | | Root Mean Square Amplitude |
| | Phonatory stability | Period perturbation, shimmer (short term, cycle-to-cycle, perturbations in the amplitude of the voice): local shimmer, amplitude perturbation quotient |
| Voice Quality | Noise | Harmonic-to-Noise Ratio |
| | | Noise-to-Harmonic Ratio |

Machine learning (ML) and Deep learning (DL) techniques are used for several of the above methods of detecting neurodegenerative disease. The most used methods for machine learning are support vector machines, decision trees, k-nearest neighbours, linear regression, linear discriminant analysis, neural networks, Bayesian networks and also techniques by combining several models such as bootstrap aggregating, boosting, stacking detailed [14].

To evaluate machine learning models, accuracy is most often used according to the relationship:

$$\text{Accuracy} = (\text{TP} + \text{TN}) / (\text{TP} + \text{TN} + \text{FP} + \text{FN})$$

where the values are TP - true positive, TN - true negative, FP - false positive and FN - false negative classifications.

Sensitivity (also recall) and specificity (also TNR) values are often given:

$$\text{Sensitivity} = \text{TP} / (\text{TP} + \text{FN})$$

$$\text{Specificity} = \text{TN} / (\text{TN} + \text{FP})$$

The average accuracy of AD disease classification reported in the analysed publications was 80%, with the average number of patients being 37 [11]. The following (Tab.5) lists the publications where the accuracy was greater than 90%. The acronym ANN stands for artificial neural network, CNN stands for convolutional neural network and NHR means noise-to-harmonics ratio.

Table 5. Predictive studies on early diagnosis of Alzheimer's disease.

| References | Year | Sample | Parameters | Predictive value | Analysis method |
|------------------------------|------|--------------------|--|-------------------|-----------------|
| López-de-Ipiña et al. [15] | 2013 | HC (20), AD (20) | Combination of two feature sets: emotional speech analysis (acoustic, voice quality, and duration features) and emotional temperature (prosodic and paralinguistic features) | AD: 75.2-97.7% | ANN |
| López-de-Ipiña et al. [16] | 2015 | HC (20), AD (20) | Automatic selection of spontaneous speech features and of maximum, minimum, variance, standard deviation, median, and mode average for full signal and voiced signal | AD: 87.30-92.43% | ML |
| Nasrolahzadeh et al. [17] | 2018 | HC (30), AD (30) | Higher-order spectral analysis | AD: 94.18-97.71% | ML |
| König et al. [18] | 2018 | MCI (44), AD (27) | Different combination of features extracted for every comparison | MCI vs. AD = 92%, | ML |
| López-de-Ipiña et al. [19] | 2018 | HC (187), MCI (38) | Several types of features are used to model both linear and non-linear disfluencies and speech. A total of 920 features are obtained. The best results are achieved with the 25-feature set. | MCI: 92-95% | DL - CNN |
| Martínez-Sánchez et al. [20] | 2018 | HC (98), AD (47) | Age, minimum amplitude, maximum amplitude difference, mean and standard deviation of the NHR; asymmetry; standard deviation in the first formant; formant 3 bandwidth; standard deviation of the Acoustic Voice Quality Index; tone variability; Normalized Pairwise Variability Index | AD: 92.4% | DA |

In the last two publications, there are a larger number of patients in whom they achieved results better than 90%. For AD patients, better classification accuracy was achieved by discriminant analysis (DA) of 92% in a study [20], which analysed the speech of 47 AD patients with a healthy group of 98 people. They selected the following characteristics for machine learning: age, minimum amplitude, maximum amplitude difference, mean and standard deviation, NHR; asymmetry; standard deviation in the first formant; bandwidth of formant 3; standard deviation of acoustic voice quality index; tone variability; normalized index of pair variability. To classify MCI diseases, they implemented the deep learning method with an accuracy of 92% [19]. They compared speech characteristics from 38 AD patients and a healthy control group of 187 people. They obtained 920 functions for the analysis of modelling linear and nonlinear disfluencies and speech, and by choosing 25 functions they achieved the best results.

They performed the classification using the CNN method, using conventional linear elements, as well as the Castiglioni fractal dimension and the Multiscale Permutation Entropy. They concluded that the choice of property was best using the nonparametric Mann-Whitney U-test.

For the analysis of machine learning, the authors stated in the study [10] that the results using SPECT (Single-photon emission computed tomography), PET (Positron Emission Tomography), and MRI devices are better, but they are extremely expensive and can only be performed by specialized workplaces. Speech signal analysis is cheaper and can also be performed on mobile phones. Therefore, the best approach today seems to be to perform multiple tasks and select different functions to combine into a more powerful resulting algorithm.

3 Parkinson's Disease

In the SCOPUS database, we identified review publications on Parkinson's disease [21]. The authors extracted the studies using inclusion and exclusion criteria from the PubMed and IEEEExplore databases for Parkinson's disease. A total of 209 studies focusing on PD and machine learning were analysed by February 2020. The studies were divided into methodological and clinical, and according to the method of scanning and the type of device, respectively.

In Table 6, the columns list the methods of voice, gait, hand, MRI, SPECT, PET, and CSF examinations, and the rows of the table list the numbers out of a total of 209 studies that focused on methodological studies or clinical trials, and the other two rows list the average precision of the listed methods of these studies and their standard deviation (SD). The abbreviations are SPECT: single photon emission computed tomography, PET: positron emission tomography, CSF: cerebrospinal fluid, Combo: combination of methods.

Table 6. Overview of the number of studies according to the method of scanning the device type.

| | Voice | Gait | Hand | MRI | SPECT | PET | CSF | other | Combo |
|--------------------|-------|------|------|------|-------|------|------|-------|-------|
| Methodology | 51 | 35 | 12 | 15 | 2 | 3 | 0 | 4 | 10 |
| Clinical | 4 | 16 | 4 | 21 | 12 | 1 | 5 | 6 | 8 |
| Average | 91,1 | 89,0 | 87,3 | 88,1 | 94,5 | 85,6 | 50,0 | 91,9 | 92,8 |
| SD | 8,5 | 8,5 | 6,4 | 7,7 | 4,2 | 6,8 | 0,0 | 6,4 | 5,9 |

The total number of methodological studies was 134 and their average patient sample size was 137, in contrast the number of clinical studies was only 72 but the average patient sample size was larger at 266. In the methodological studies, voice recordings were the most commonly used data modality ($n = 51$), followed by GAIT motion ($n = 35$) and then MRI data ($n = 15$). For clinical studies, MRI data were important ($n = 21$), followed by GAIT ($n = 16$) and then SPECT ($n = 12$). The average accuracy achieved across studies for each data type was highest for SPECT (94.5%) and a combination of multiple methods (92.8%) and voice recording (91.1%). The following Figure 1 shows the average accuracy for the defined modalities and their standard deviations in the reported studies.

In terms of the frequency of use of machine learning methods in selected PD studies, Mei et al. [21] divided these methods into the following types: SVM, support vector machine; NN, neural network; EL, ensemble learning; k-NN, nearest neighbour; regr, regression; DT, decision tree; NB, naive Bayes; DA, discriminant analysis; other, data/models. Figure 2 shows the percentage of machine learning methods used for Voice, Gait and Hand adopted from [21].

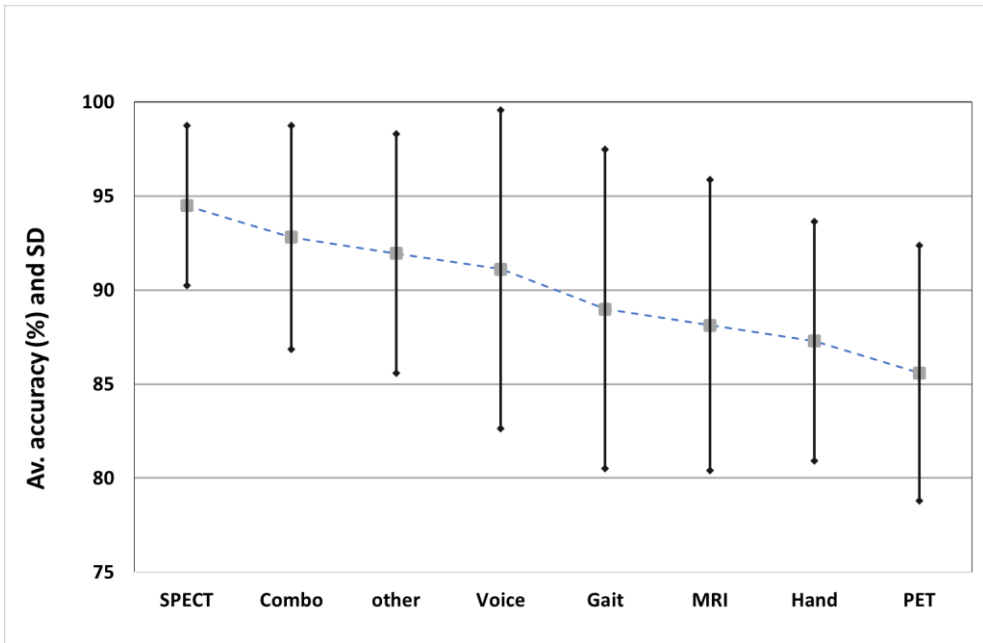


Figure 1. Average accuracy for a given modality with standard deviation for selected studies reported in [21].

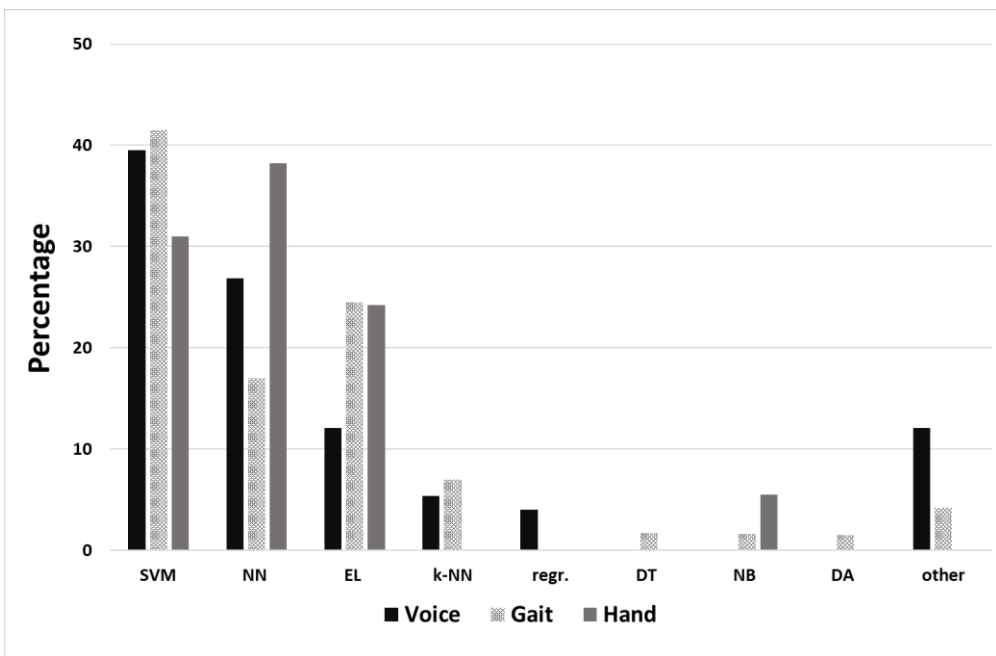


Figure 2. Frequency of machine learning methods for Voice, Gait, and Hand.

Some studies for the Hand measured mobile phone movement in patients with PD. The resulting machine learning qualifiers using neural networks achieved 95% accuracy (see Figure 2). These results suggest that the mobile phone accelerometer can accurately detect vibrational motion in PD patients.

The following Table 7 selects publications from the Voice dataset ($n = 55$) in which the number of patients with PD was at least 40 and the accuracy or one of the sensitivity and accuracy values was greater than 90% [21].

Table 7. Publications according to criteria: number of PD > 40 a (Accuracy or Sensitivity or Precision) > 90%

| References | Year | Sample | Analysis method | Predictive value |
|---------------------------|------|--------------------|---|---|
| Erdogdu Sakar et al. [22] | 2017 | PD(42) + HC(8) | KNN, SVM, ELM with train-validation ratio of 70:30 | Accuracy = 96,4% |
| Sztaho et al. [23] | 2019 | PD(55) + HC(33) | KNN, SVM-linear, SVM-RBF, ANN, DNN with leave-one-subject-out cross validation | Accuracy = 89,3% Sensitivity = 90,2% |
| Tracy et al. [24] | 2019 | PD(246) + HC(2023) | regression, random forest, gradient boosted decision trees with 5-fold cross validation | Precision = 90,1% |
| Wodzinski et al. [25] | 2019 | PD(50) + HC(50) | ResNet with train-validation ratio of 90:10 | Accuracy = 91,7% Precision = 92,0% |
| Yaman et al. [26] | 2020 | PD(40) + HC(40) | KNN, SVM with 10-fold cross | Accuracy = 91,3% Precision = 91,3% |

4 Discussion

The Early Warning of Alzheimer (EWA) project is concerned with the early detection of Alzheimer's and Parkinson's diseases [27]. The project is implemented by researchers from AXON PRO, the Institute of Informatics of the Slovak Academy of Sciences and the Faculty of Informatics of the Pan-European University together with doctors from the Faculty of Medicine of the P. J. Šafárik University. Within the framework of the project, a mobile application for automatic detection was developed for the collection of speech data of healthy people and patients with neurodegenerative diseases for automatic detection of AD and PD with some accuracy. The speech recording system was designed using image naming and verbal description of images being similar to the well-known picture "Cookie Theft" (new version Stealing Cookies in [28]). In the following, we briefly describe the process of acquiring the data needed to best predict AD and PD.

According to the proposed procedure, patients diagnosed with AD and PD are closely monitored for how they respond to the displayed pictures, and their spontaneous speech is recorded either at the MEMORY Centre for AD or at the Neurology clinic for PD. In the case of diagnosed patients, all available information in addition to medical history is used to make an accurate diagnosis. Three selected psychological tests are also administered: the Montreal Cognitive Assessment (MoCA), the Beck Depression Inventory (BDI), and the Generalized Anxiety Disorder (GAD-7). According to the above scenario, audio recordings of picture descriptions as well as the MoCA, BDI, and GAD-7 tests are also recorded for a healthy control of the population.

The audio recordings were processed using specialized software and a suitable feature selection algorithm for speech and sound processing, which was developed at the Institute of Informatics of the Slovak Academy of Sciences in Bratislava. Preliminary experiments indicate that recordings of patients' spontaneous speech in Slovak while describing pictures using a mobile app may also reveal subtle changes in the voice of people with neurodegenerative diseases, which will help in early detection of AD and PD.

As can be seen from the tables presented in the previous sections of this paper, many of the machine learning applications in the reviewed papers relied on relatively small amounts of collected data. Obtaining data from a large group of clinical trial participants is critical for the most accurate predictions, which is what we are trying to accomplish in our EWA project. Data collected from Alzheimer's and Parkinson's patients and a group of healthy people are evaluated using special artificial intelligence algorithms to best determine accuracy, sensitivity, and specificity.

Conclusion

Patients with suspected Alzheimer's and Parkinson's disease need to be identified as early as possible so that treatment can be started early, and the patient's disease progresses as little as possible. Results up to date show that the detection of neurodegenerative diseases using automated analysis of human voice and speech can be achieved with an accuracy of more than 90% under laboratory conditions. As we showed in Table 7, the sensitivity of disease prediction can reach more than 90% depending on the selected group of patients and healthy people, the processing of spontaneous speech of this group, and finally the algorithms and methods of artificial intelligence.

Acknowledgement

This paper was supported by Operational Program Integrated Infrastructure co-financed by the European Regional Development Fund under contract number 67/2020-2060-2230-V631.

References

- [1] WHO. (2021). WHO reveals leading causes of death and disability worldwide: 2000-2019. Retrieved June 2021, from <https://www.who.int/news/item/09-12-2020-who-reveals-leading-causes-of-death-and-disability-worldwide-2000-2019>
- [2] NCZI, Národné centrum zdravotných informácií. (2021). ZDRAVOTNÍCKA ROČENKA. HEALTH YEARBOOK. Retrieved June 2021, from: http://www.nczisk.sk/statisticke_vystupy/zdravotnicka_rocenka/Pages/default.aspx
- [3] Boschi, V, Catricalà, E, Consonni, M, Chesi, C, Moro, A, Cappa, S.F. (2017). Connected Speech in Neurodegenerative Language Disorders: A Review. *Front. Psychol.* 8:269. doi: 10.3389/fpsyg.2017.00269
- [4] Sajjadi, S. A., Patterson, K., Tomek, M., and Nestor, P. J. (2012). Abnormalities of connected speech in semantic dementia vs. Alzheimer's disease. *Aphasiology* 26, p. 847–866
- [5] Hoffmann, I., Nemeth, D., Dye, C. D., Pákási, M., Irinyi, T., and Kálmán, J. (2010). Temporal parameters of spontaneous speech in Alzheimer's disease. *Int. J. Speech Lang. Pathol.* 12, p. 29–34.
- [6] Goberman, A. M., and Coelho, C. (2002). Acoustic analysis of Parkinsonian speech I: speech characteristics and L-Dopa therapy. *Neurorehabilitation* 17, p. 237–246.

- [7] Ash, S., McMillan, C., Gross, R. G., Cook, P., Gunawardena, D., Morgan, B., et al. (2012). Impairments of speech fluency in Lewy body spectrum disorder. *Brain Lang.* 120, p.290–302.
- [8] Rusz, J., Cmejla, R., Ruzickova, H., and Ruzicka, E. (2011). Quantitative acoustic measurements for characterization of speech and voice disorders in early untreated Parkinson's disease. *J. Acoust. Soc. Am.* 129, 350–367.
- [9] Crescentini, C., Mondolo, F., Biasutti, E., and Shallice, T. (2008). Supervisory and routine processes in noun and verb generation in nondemented patients with Parkinson's disease. *Neuropsychologia* 46, 434–447. doi: 10.1016/j.neuropsychologia.2007.08.021
- [10] Pulido, M.L.B., Hernández, J.B.A., Ballester, M.Á.F., González, C.M.T., Mekyska, J., and Smékal, Z. (2020). Alzheimer's disease and automatic speech analysis: A review. *Expert Systems with Applications*, 2020, vol. 150, p. 113-213
- [11] Martínez-Nicolás, I., Llorente, T.E., Martínez-Sánchez, F., and Meilán, J.J.G. (2021). 'Ten Years of Research on Automatic Voice and Speech Analysis of People With Alzheimer's Disease and Mild Cognitive Impairment: A Systematic Review Article', *Front Psychol*, 2021, vol. 12, p. 620251-620251.
- [12] Laske, C., Sohrabi, H.R., Frost, S.M., López-de-Ipiña, K., Garrard, P., Buscema, M., et al. (2015). 'Innovative diagnostic tools for early detection of Alzheimer's disease', *Alzheimer's & dementia : the journal of the Alzheimer's Association*, 2015, 11, (5), p. 561-578
- [13] Hane, F.T., Robinson, M., Lee, B.Y., Bai, O., Leonenko, Z., and Albert, M.S. (2017). 'Recent Progress in Alzheimer's Disease Research, Part 3: Diagnosis and Treatment', *Journal of Alzheimer's disease : JAD*, 2017, 57, (3), p. 645-665
- [14] Kuhn, M. and Johnson, K. (2019). *Applied predictive modeling*. New York, NY: Springer, 2019.
- [15] López-de-Ipiña, K., Alonso, J.B., Travieso, C.M., Solé-Casals, J., Egiraun, H., Faundez-Zanuy, M., et al. (2013). 'On the selection of non-invasive methods based on speech analysis oriented to automatic Alzheimer disease diagnosis', *Sensors (Basel, Switzerland)*, 2013, vol. 13, (5), p. 6730-6745
- [16] López-de-Ipiña K., Alonso-Hernández J. B., Solé-Casals J., Travieso-González C. M., Ezeiza A., Faundez-Zanuy M., et al. . (2015). Feature selection for automatic analysis of emotional response based on nonlinear speech modeling suitable for diagnosis of Alzheimer's disease. *Neurocomputing* 150, p. 392–401. doi: 10.1016/j.neucom.2014.05.083
- [17] Nasrolahzadeh, M., Mohammadpoori, Z., Haddadnia, J. (2018). Higher-order spectral analysis of spontaneous speech signals in Alzheimer's disease. *Cogn. Neurodyn.* 12, p. 583–596. doi: 10.1007/s11571-018-9499-8
- [18] König, A., Satt, A., Sorin, A., Hoory, R., Derreumaux, A., David R., et al. (2018). Use of speech analyses within a mobile application for the assessment of cognitive impairment in elderly people. *Curr. Alzheimer Res.* 15, p. 120–129. doi: 10.2174/1567205014666170829111942
- [19] López-de-Ipiña, K., Martínez-de-Lizarduy, U., Calvo, P. M., Beitia, B., García-Melero, J., Fernández E., et al. . (2018). On the analysis of speech and disfluencies for automatic detection of Mild Cognitive Impairment. *Neural Comput. Appl.* 32, p. 15761–15769. doi: 10.1007/s00521-018-3494-1
- [20] Martínez-Sánchez, F., Meilán, J. J. G., Carro, J., Ivanova, O. (2018). A prototype for the voice analysis diagnosis of Alzheimer's disease. *J. Alzheimers. Dis.* 64, p. 473–481. doi: 10.3233/JAD-180037
- [21] Mei, J., Desrosiers, C., and Frasnelli, J. (2021). 'Machine Learning for the Diagnosis of Parkinson's Disease: A Review of Literature'. *Frontiers in Aging Neuroscience*. 2021, vol. 13, p. 184-201. doi: 10.3389/fnagi.2021.633752
- [22] Erdogdu Sakar, B., Serbes, G., and Sakar, C. O. (2017). Analyzing the effectiveness of vocal features in early teliagnosis of Parkinson's disease. *PLoS ONE* 12:e0182428. doi: 10.1371/journal.pone.0182428
- [23] Sztahó, D., Valálik, I., and Vicsi, K. (2019). "Parkinson's disease severity estimation on Hungarian speech using various speech tasks," in 2019 International Conference on Speech Technology and Human-Computer Dialogue (SpeD) (Timisoara), 1–6. doi: 10.1109/SPED.2019.8906277

- [24] Tracy, J. M., Özkanca, Y., Atkins, D. C., and Hosseini Ghomi, R. (2019). Investigating voice as a biomarker: deep phenotyping methods for early detection of Parkinson's disease. *J. Biomed. Inform.* 104:103362. doi: 10.1016/j.jbi.2019.103362
- [25] Wodzinski, M., Skalski, A., Hemmerling, D., Orozco-Arroyave, J. R., and Nöth, E. (2019). "Deep learning approach to Parkinson's disease detection using voice recordings and convolutional neural network dedicated to image classification," In 2019 41st Annual International Conference of the IEEE Engineering in Medicine and Biology Society (EMBC) (Berlin), p. 717–720. doi: 10.1109/EMBC.2019.8856972
- [26] Yaman, O., Ertam, F., and Tuncer, T. (2020). Automated Parkinson's disease recognition based on statistical pooling method using acoustic features. *Med. Hypoth.* 135:109483. doi: 10.1016/j.mehy.2019.109483
- [27] Early Warning of Alzheimer (2021). Project of Operational Program Integrated Infrastructure Retrieved September 2021, from <https://www.paneurouni.com/veda/najvyznamnejsie-projekty-a-granty/early-warning-of-alzheimer/>
- [28] Berube, S., Nonnemacher, J., Demsky, C., Glenn, S., Saxena, S., Wright, A., Tippett, D. C., Hillis, A. E. (2019). Stealing Cookies in the Twenty-First Century: Measures of Spoken Narrative in Healthy Versus Speakers with Aphasia. *American journal of speech-language pathology*, 28(1S), 321–329. https://doi.org/10.1044/2018_AJSLP-17-0131.

▲ Authors

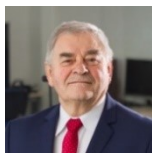


Assoc. Prof. RNDr. Eugen Ružický, PhD.

Faculty of Informatics, Pan-European University, Bratislava, Slovakia

eugen.ruzicky@paneurouni.com

His research interests include Applied informatics, System analysis, Modelling, Visualisation and Applications in Medicine.



prof. Ing. Štefan Kozák, PhD.

Faculty of Informatics, Pan-European University, Bratislava, Slovakia

stefan.kozak@paneurouni.com

His research interests include system theory, linear and nonlinear control methods, numerical methods and software for modeling, control, signal processing, IoT, IIoT and embedded intelligent systems for digital factory in industry and medicine.



RNDr. Ján Lacko, PhD.

Faculty of Informatics, Pan-European University, Bratislava, Slovakia

jan.lacko@paneurouni.com

His research interests include digitization of objects from the field of cultural heritage, healthcare, industry, urban planning and their display by various techniques, including virtual and augmented reality.



Ing. Juraj Štefanovič, PhD.

Faculty of Informatics, Pan-European University, Bratislava, Slovakia

juraj.stefanovic@paneurouni.com

His research interests include modeling and simulation of discrete systems in technology applications.



RNDr. Alfréd Zimmermann

He is owner and CEO of the company. Professional and scientific interests include AI in general and NLP.
AXON PRO Ltd.
zimmermann@axonpro.sk



Ing. Milan Rusko, PhD.

Head of the Department of Speech Analysis and synthesis, project manager and researcher at Institute of Informatics, Slovak Academy of Sciences. Expertise in acoustics, artificial intelligence, speech synthesis, speech, speaker and emotion recognition.
Institute of Informatics, Slovak Academy of Sciences, Bratislava, Slovakia
utrusrusk@savba.sk



Mgr. Petra Brandoburová, PhD.

Her research interests include clinical neuropsychology of adults with a main focus on the early detection of neurodegenerative diseases.
Department of Psychology, Comenius University, Bratislava, Slovakia
MEMORY Centre n.g.o., Bratislava, Slovakia
petra.brandoburova@uniba.sk



Assoc. Prof. Matej Škorvánek, MD, PhD.

His research interest is related mainly to assessment of prodromal, non-motor and genetic aspects of Parkinson's disease, advanced therapeutic options for movement disorders and rare hyperkinetic movement disorders.
Dept. of Neurology and Center for Rare Movement Disorders,
University of P. J. Safarik, Kosice, Slovakia
mskorvanek@gmail.com

STATISTICAL MECHANICS OF COMPLEX GRAPHS

David Šablatúra

Abstract:

Modelling of graphs as abstract mathematical structures is often utilised in myriad of studies across the whole spectrum of scientific fields. This paper aims to investigate some of the graph theory characteristics of complex systems. Such investigation is applicable for real-world phenomena studies and optimisation simulations of models representable by graph theory structures. A random model generation algorithm was developed to build random graphs that were further perturbed by adding edges according to a custom preferential edge attachment algorithm. The edge attachment algorithm forces nodes in the model to coalesce into large but fewer components. Analysis of the analytically validated model graph structures by means of node degree histograms supports the proposed behaviour of graphs upon new edge addition.

Keywords:

Complex graphs, node degree, graph theory, graph and network algorithms, MATLAB.

ACM Computing Classification System:

Mathematics of computing, discrete mathematics, graph theory, random graphs.

Introduction

Graph mechanics, as both a theoretical and a practical background, constitute to various phenomena in physics, medicine, chemistry, biology, social sciences, transport systems etc. (Palko, 2017). Economics, pollution, epidemics are only a tip of the iceberg areas where graphs can be utilized to study the relationships and dynamics in complex systems. Substantial amount of research was done around small world networks, theory of which postulates that even in apparently complex network structures, the average distance between nodes remains unexpectedly small as that is analytically proportional to the logarithm of the number of nodes (Pelánek, 2011. Štefanovič, 2021). Barabási summarised networks with various average path lengths (Réka et Barabási, 2002). Existing models of graph manipulation were studied. Evolving models for preferential and random evolution, both for edge and node addition are well described in literature (Blum et al. 2020. Réka et Barabási, 2002).

A simple random graph generator algorithm was developed, implemented, and validated against theoretical concepts from literature. Preferential node attachment algorithm was developed, which manifested in nodes to components coalescence. Such pseudo-random graph's properties were subsequently analyzed.

1 Graph Model Specification

Seemingly similar applications of graph theory might exhibit contradictory graph properties. For example, a network of Facebook users is an undirected graph as relations are defined by friendships, on the other hand Twitter and Instagram user base network is specified by who is following who, only representable by directed graphs. It is therefore important to understand these properties prior to accepting model assumptions. In this paper, the following standard notation will be used to represent basic graph properties, where by definition, an undirected graph is representable by any two of the three:

- n - number of nodes
- e - number of edges
- R - ratio: number of edges / number of nodes

For each undirected graph, the maximum number of edges is bounded by the number of nodes

$$0 < R < \binom{n}{2} = \frac{n-1}{2} \quad (1)$$

A custom algorithm implemented to generate random graph structures was used such that for a specified input set of parameters (e.g. number of nodes $n = 30$ and ratio of edges to nodes $R = 0.5$), an $n \times n$ adjacency matrix G is created. Each new edge, connecting two nodes, is then allocated to the i -th row and k -th column from those node pair combinations, that do not already have an edge connecting them. In practice, the algorithm looks for a random 0, representing an absence of an edge for the ordered pair of nodes combination. The non-existence of a node is often represented by a value of “Inf” (∞) instead of a “0”, which is inevitable in analysis involving weighted graphs. Since this paper focuses on pseudo-static statistical graph analysis and no node-to-node distances are calculated, it is adequate to consider undirected graphs only. Hence only upper right triangle of the adjacency matrix is considered. By representing edges of weight “1” (“exists”) only and excluding the matrix diagonal, the model only represents irreflexive, undirected (symmetric) unweighted graphs (Blum et al. 2020, Thulasiraman et al. 2016).

To enable analysis of the components, disconnected subgraphs in a graph, a MATLAB built-in function – `concomp()` was utilised. Which returned indexes of components per each node in the graph. After postprocessing this data, the custom source code prints the following console output:

```

Console output: Graph components
=====
An adjacency matrix was created
Number of nodes:30
Number of edges:15
edges/nodes:0.5
=====
Number of Components = 16
All these nodes are connected: 1 7 24
All these nodes are connected: 2
All these nodes are connected: 3 4 5 8 11 20 23 26
All these nodes are connected: 6
All these nodes are connected: 9 12 16
All these nodes are connected: 10 27
All these nodes are connected: 13
All these nodes are connected: 14
All these nodes are connected: 15
All these nodes are connected: 17

```

```

All these nodes are connected: 18 22
All these nodes are connected: 19 25
All these nodes are connected: 21
All these nodes are connected: 28
All these nodes are connected: 29
All these nodes are connected: 30
=====
Model test, nodes in components == nodes in graph :30 == 30
This many COMPONENTS:      1x      2x      3x      10x      |
have got this many nodes:  8n      3n      2n      1n      | SUM=30nodes
=====
    
```

As presented in (Fig.1), the generated graph structure satisfies the requirements for number of edges and nodes. Double checked by comparing the summation from component nodes and overall graph number of nodes. As a result of true random graph properties, sixteen individual components were created as the nodes coalesced in the process of adding edges. Comprised of ten components each with one node, three components with two nodes each, two components with two nodes each and a one component with eight nodes, overall thirty nodes.

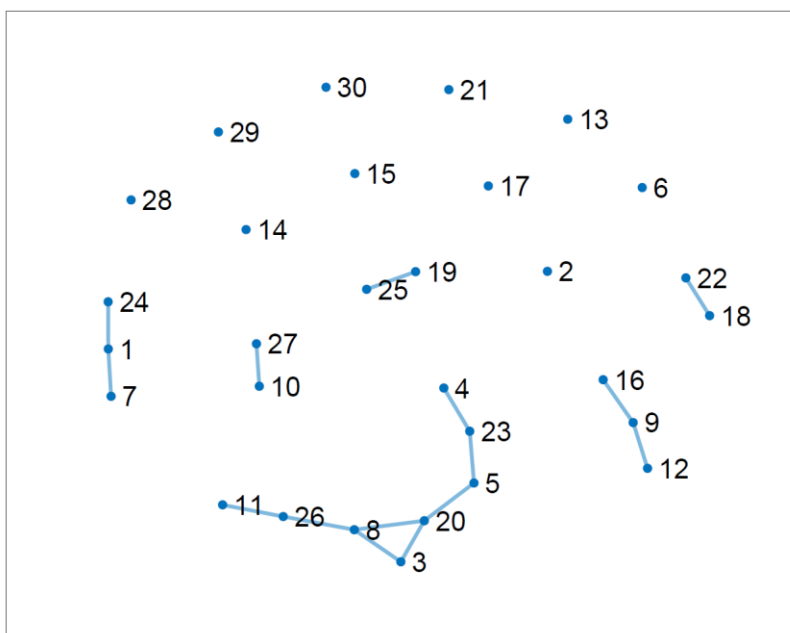


Fig.1. Structure of the generated random Graph, $n=30$, $e=15$.

Multiple graphs with $n = 1000$ and $R = 0.5, 1, 1.5$ were constructed this way, which yielded in the node – edge distribution in (Fig.2). Calculated as a histogram of the column-wise summations from the adjacency matrix. Due absence of directed edges, number of edges distribution is equivalent to the node total degree distribution as there are no directional node in/out-degrees defined.

Edge probability distribution as a function of the node 1-degree number

For all nodes in the graph, it is useful to first find the number of its closest 1-edge neighbours. The algorithm for calculation of the node degree number involves the aforementioned column-wise summation of the number of existing nodes for each i -th node – column.

For example, the first node has got 2 one-edge neighbours (node degree of two) and there are only 2 nodes, that have node degree of 3 (8th and 20th nodes) as evidenced in (Fig.3). The node degrees are stored in a vector A , presented in Console output below.

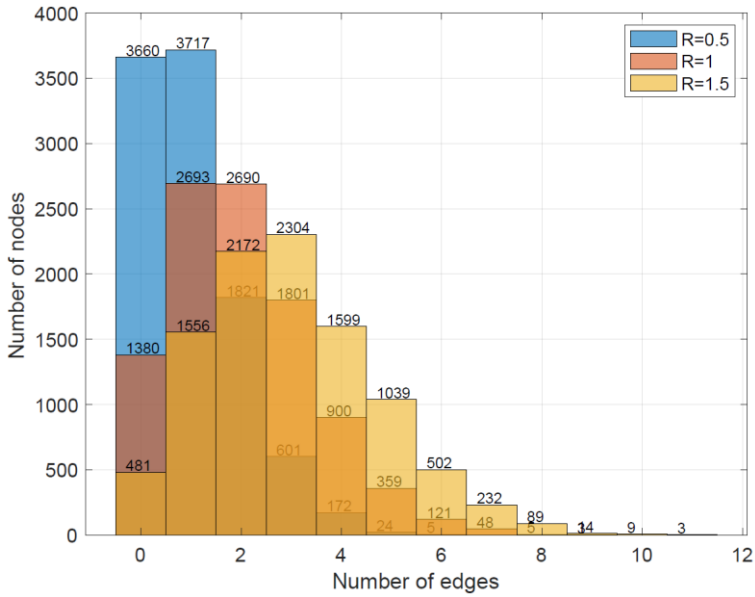


Fig.2. Edge degree distribution. (see online journal for coloured graph)

| Console output: Vector A (30 nodes) | | | | | | | | | |
|-------------------------------------|---|---|---|---|---|---|---|---|---|
| $A = 2$ | 0 | 2 | 1 | 2 | 0 | 1 | 3 | 2 | 1 |
| 1 | 1 | 0 | 0 | 0 | 1 | 0 | 1 | 1 | 3 |
| 0 | 1 | 2 | 1 | 1 | 2 | 1 | 0 | 0 | 0 |

Before the next step, unity is added to the vector, to ensure a useful property exploited later, $A = A + 1$.

| Console output: Vector A (30 nodes) | | | | | | | | | |
|-------------------------------------|---|---|---|---|---|---|---|---|---|
| $A = 3$ | 1 | 3 | 2 | 3 | 1 | 2 | 4 | 3 | 2 |
| 2 | 2 | 1 | 1 | 1 | 2 | 1 | 2 | 2 | 4 |
| 1 | 2 | 3 | 2 | 2 | 3 | 2 | 1 | 1 | 1 |

The probability of an existing i -th node to gain a new friendship to another existing node is then rationed based on these numbers. It is a probability distribution B_k defined by relative node degrees(+1). Analytically obtained by equation $B_k = A_k / \sum A$.

| Console output: Vector B (30 nodes) | | | | | |
|-------------------------------------|--------|--------|--------|--------|--------|
| $B = 0.0500$ | 0.0167 | 0.0500 | 0.0333 | 0.0500 | 0.0167 |
| 0.0333 | 0.0667 | 0.0500 | 0.0333 | 0.0333 | 0.0333 |
| 0.0167 | 0.0167 | 0.0167 | 0.0333 | 0.0167 | 0.0333 |
| 0.0333 | 0.0667 | 0.0167 | 0.0333 | 0.0500 | 0.0333 |
| 0.0333 | 0.0500 | 0.0333 | 0.0167 | 0.0167 | 0.0167 |

To enable an index selection based on these relative probabilities, cumulative probability property is used, by splitting the interval of $\langle 0,1 \rangle$ to n intervals based on $O_k = \sum_{i=1}^k B_i$.

| Console output: Vector O (30 nodes) | | | | | |
|-------------------------------------|--------|--------|--------|--------|--------|
| o = 0.0500 | 0.0667 | 0.1167 | 0.1500 | 0.2000 | 0.2167 |
| 0.2500 | 0.3167 | 0.3667 | 0.4000 | 0.4333 | 0.4667 |
| 0.4833 | 0.5000 | 0.5167 | 0.5500 | 0.5667 | 0.6000 |
| 0.6333 | 0.7000 | 0.7167 | 0.7500 | 0.8000 | 0.8333 |
| 0.8667 | 0.9167 | 0.9500 | 0.9667 | 0.9833 | 1 |

A randomly generated number from $\langle 0,1 \rangle$ is always smaller or equal to at least one of the O numbers. The source code identifies the first of the numbers k such that the O_k satisfies the condition. Resulting in that node index number k . Distribution of these node degree generated node index numbers is perfectly correlated to the number of closest neighbours – node degree numbers. The node with this index number is then allocated a new random probability defined edge (P-edge) to any other node not yet interconnected with k -th node. For example even a node from its existing component. The unity was added to the A matrix to aid node addition to those nodes, that are individually standing components, that is nodes with the degree 0. Otherwise these 0-degree nodes could have had new edges added only if another non-0-degree nodes were already selected and the 0-degree nodes were added randomly in the step 2 as an undirected *edge-end* node. The probability of a new edge in an empty n node graph would have been 0.

The algorithm is demonstrated in following Figures, where for a random graph with 30 nodes and the initial edges to nodes ratio of 0.5 P-edges were added (Fig.3).

At first, the node 26 is selected based on its initial relative degree number of 2. And then, randomly selected non-existing connection is made, with node 10, which is in a separate 2 node component. Therefore, in this case, an addition of one edge means addition of two nodes, see (Fig.4) This can vary from 0 nodes when connecting to a node within the component to the maximum component size in other graph components.

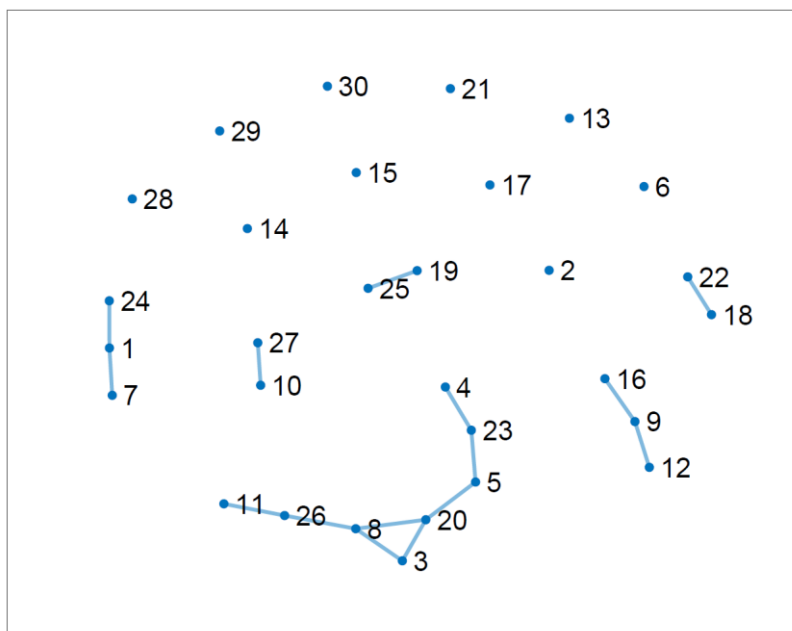


Fig.3. Structure of the generated random Graph, $n=30, e=15$.

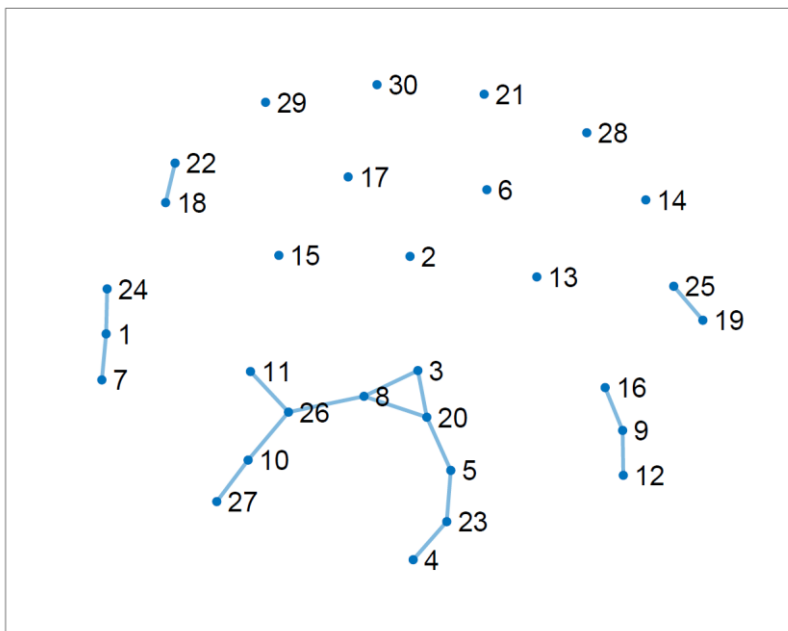


Fig.4. Structure of the generated Graph with an extra P-edge, $n=30$, $e=16$.

Repeating this 14 more times, a graph in (Fig.5) with a master component was obtained.

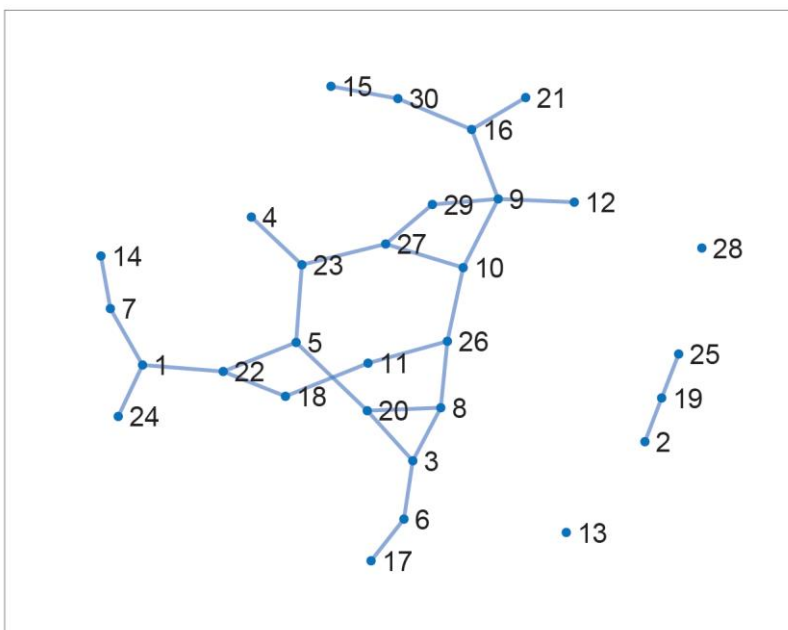


Fig.5. Structure of the generated Graph with an extra P-edge, $n=30$, $e=30$.

The output of the program successfully identifies node relations to the components, as viewed in console output below.

```

Console output: Graph components
=====
Number of Components = 4
All these nodes are connected: 1 3 4 5 6 7 8 9 10 11 12 14 15 16 17 18 20 21 22
23 24 26 27 29 30
All these nodes are connected: 2 19 25
All these nodes are connected: 13
All these nodes are connected: 28
=====
Model test, nodes in components==nodes in graph :30==30
This many COMPONENTS:      1x      1x      2x      |
have got this many nodes:  25n     3n      1n      |  SUM=30nodes
=====
    
```

As presented in (Fig.5), an addition of edges based on the degree of the nodes, a master component quickly emerges.

For a number of nodes $n = 1000$ and original number of edges $e = 500$, (Fig.6), it is clear that after increasing the edges to nodes ratio from $R = 0.5$ to $R = 0.7$, the number of nodes in the largest component size rapidly increases, (Fig.7).

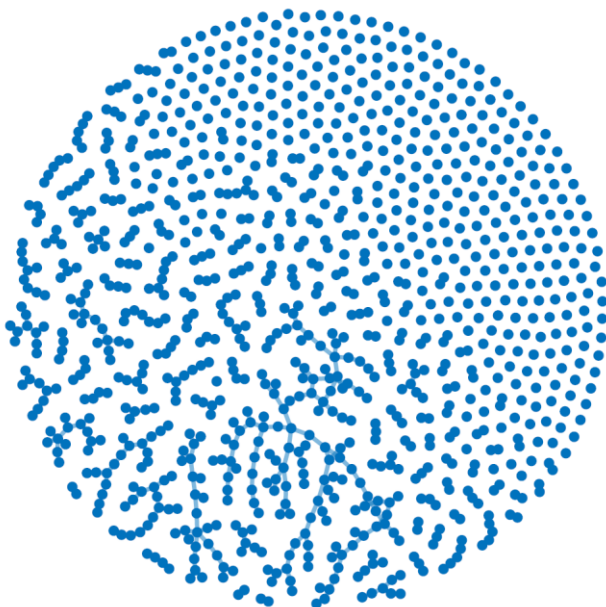


Fig.6. $n=1000, e=500$.

The discrepancy between structure of the graph in (Fig.7) generated by having 500 random edges and additional 200 node degree probability defined edges and a random graph with no P-edges, but 700 random edges instead, is small but not negligible, as evidenced in (Fig.8).

This is an interesting finding, as the distribution of a truly random graph highly correlates to the distribution of an initially lighter graph (less edges) with added nodes according to the custom node degree derived algorithm.

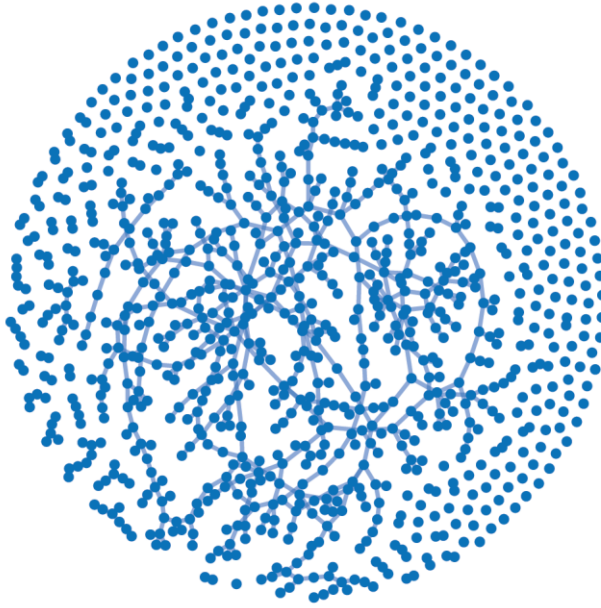
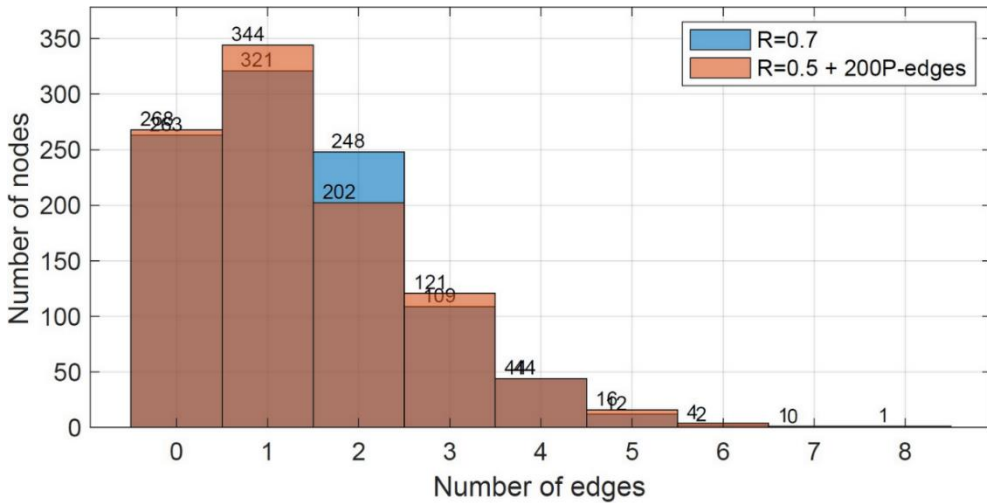
Fig.7. $n=1000$, $e=500 + 200$ P-edges.

Fig.8. Node degree distributions for two graphs both with $n=1000$, $e=700$ (edges to nodes ratio $R=0.7$)
orange graph has got original $R=0.5$ and 200 extra Preferential edges.

Generally, the first node in the new node pair in custom P-edge algorithm is selected according to the node degree relative number and the other to create the edge is selected randomly from nodes it is not already connected with. Whereas truly random graph algorithm selects all non-existent edges (unordered node pairs). The comparison of the calculations below, show discrepancy in one of the new edge nodes probability distributions.

$$G(n = 5, e = 12) = \begin{bmatrix} 0 & 1 & 0 & 1 & 1 \\ 1 & 0 & 1 & 1 & 0 \\ 0 & 1 & 0 & 0 & 0 \\ 1 & 1 & 0 & 0 & 1 \\ 1 & 0 & 0 & 1 & 0 \end{bmatrix}$$

Probability of the node becoming a new edge source node:

| | |
|---|--|
| $A(G = 1) = [3 \ 3 \ 1 \ 3 \ 2]$ $A + 1 = [4 \ 4 \ 2 \ 4 \ 3], \sum A + 1 = 17$ $P_{\text{new P-edge}} = \left[\frac{4}{17}, \frac{4}{17}, \frac{2}{17}, \frac{4}{17}, \frac{3}{17} \right]$ | $A(G = 0)_{\text{irreflexive}} = [1 \ 1 \ 3 \ 1 \ 2], \sum A = 8$ $P_{\text{new random edge}} = \left[\frac{4}{8}, \frac{4}{8}, \frac{2}{8}, \frac{4}{8}, \frac{3}{8} \right]$ |
|---|--|

The specific probability distributions for this graph structure are visualised in (Fig.9). Although probabilities for individual nodes may vary significantly, the resulting structures are not too dissimilar.

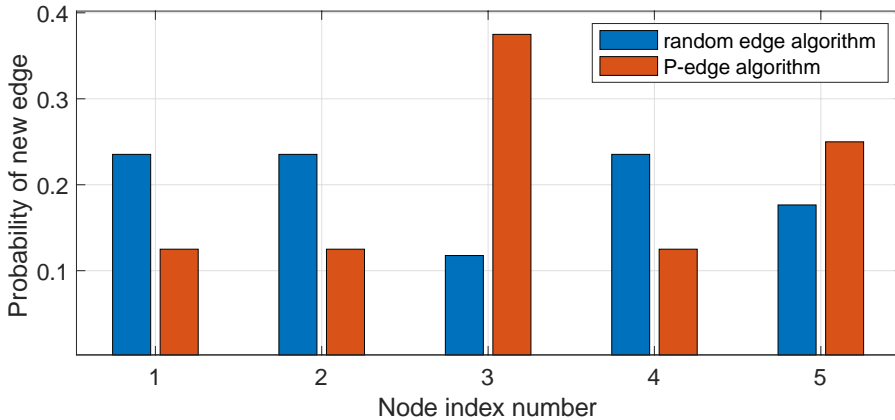


Fig.9. Probability of the node acting as an undirected edge source. (P-edge = preferential edge algorithm generated, it is every second column)

2 Stability of Solution

Upon repeated execution of the P-edges algorithm, for identical input settings with number of nodes $n = 1000$ and number of edges $e = 500$, the algorithm of the P-edge allocation produces similar graph structures, observed in (Fig.10). Curves for data1 through data7 depict 7 independent simulation runs.

(Fig.11) demonstrates the same data, both axes were adjusted to logarithmic scale. The apparent linearity in the log-log axes, demonstrates the inverse proportionality such that number of nodes $n \propto$ inverse of the number of graph components and vice versa.

Detailed analysis of a larger number of nodes graphs at various edge to node ratios led to a conclusion that the simulation of the node relationships with this Monte Carlo probability method leads to expected results and deducing from that, the model is valid.

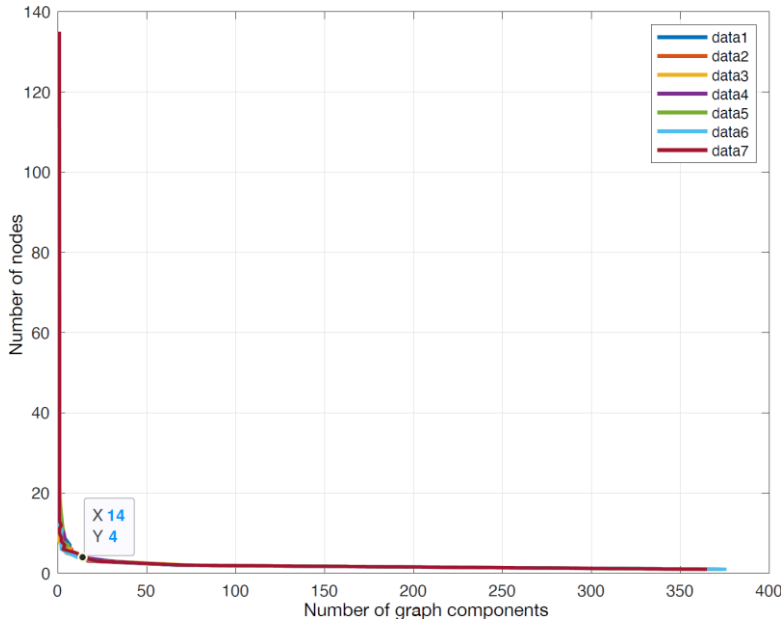


Fig.10. Distribution of the number of components versus number of nodes for an initial graph with $n=1000$, $e=500$ and additional 100 P-edges.

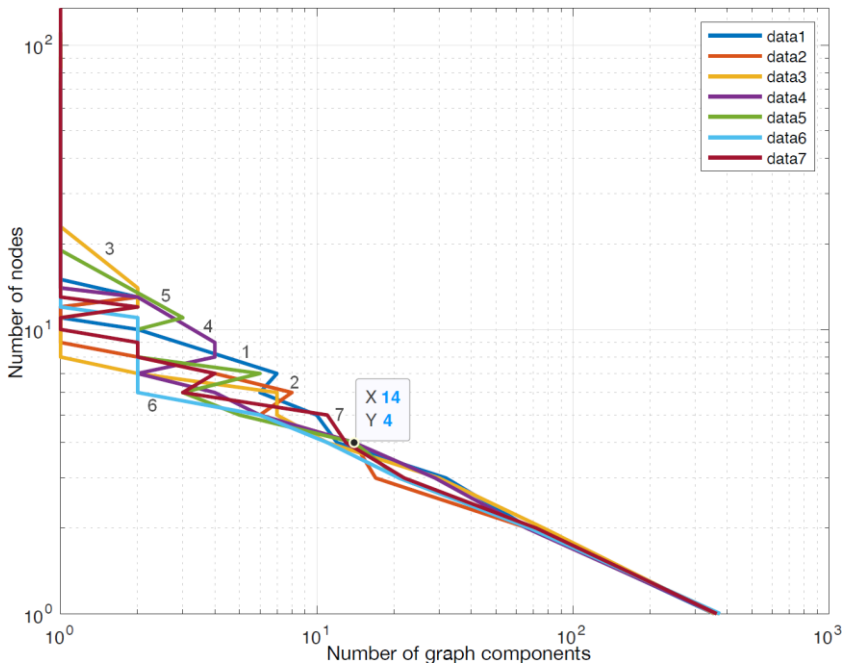


Fig.11. DETTO log-log distribution of the number of components versus number of nodes for an initial graph with $n=1000$, $e=500$ and additional 100 P-edges. (refer to the online journal issue in colour)

3 Large Graph Analysis

In this section, the percentage fraction of the individually standing nodes (one node components, 0-degree nodes) is the primary observed quantity. The independent variables are number of nodes and number of edges.

A randomly generated graph with a specific number of nodes n and an edges to nodes ratio of $R = 0.5$, will always have 36 – 37% of its nodes with node degree of 0. In other words, the 36% of the nodes are individually standing components. This is has been demonstrated both analytically and experimentally. The experiment results are presented in the (Table 1).

Table 1. Convergence of the fraction of the individually standing nodes in graphs with R=0.5

| Number of nodes | 0-degree nodes | Number of edges |
|-----------------|----------------|-----------------|
| 10 | 30% | 5 |
| 100 | 39% | 50 |
| 1000 | 36.1% | 500 |
| 10000 | 36.38% | 5000 |
| 15000 | 5538=36.92% | 7500 |

Analogously, the analysis for the edges to nodes ratio of $R = 0.8$, resulted in a fraction of apprximately 20% of the nodes standing individually, (Table 2).

Table 2. Convergence of the fraction of the individually standing nodes in graphs with R=0.8

| Number of nodes | 0-degree nodes | Number of edges |
|-----------------|----------------|-----------------|
| 10 | 2 | 8 |
| 100 | 19 | 80 |
| 1000 | 216 | 800 |
| 10000 | 2034 | 8000 |
| 15000 | 3023 | 12000 |

The fraction of individually standing nodes in random graphs with an edges to nodes ratio $R = 1.1$ converges to around 11%, (Table 3).

Table 3. Convergence of the fraction of the individually standing nodes in graphs with R=1.1.

| Number of nodes | 0-degree nodes | Number of edges |
|-----------------|----------------|-----------------|
| 10 | 1 | 11 |
| 100 | 12 | 110 |
| 1000 | 106 | 1100 |
| 10000 | 1122 | 11000 |
| 15000 | 1655 | 16500 |

Finally, various simulations with a large number of nodes are summarised in the (Table 4). Presented graphically in (Fig.12). The relationship is logarithmic as validated in following paragraphs.

$$\log\left(\frac{0 - \text{degree nodes}}{n \text{ number of nodes}}\right) \propto R$$

Table 4. Number of 0-degree nodes as a function of edges to nodes ratio R.

| Number of nodes | 0-degree nodes | Edges to nodes ratio R |
|-----------------|----------------|------------------------|
| 30000 | 11028 | 0.5 |
| 30000 | 9013 | 0.6 |
| 30000 | 6063 | 0.8 |
| 30000 | 4955 | 0.9 |
| 30000 | 4056 | 1 |
| 30000 | 3346 | 1.1 |
| 30000 | 1888 | 1.4 |
| 30000 | 1122 | 1.6 |
| 30000 | 637 | 1.9 |

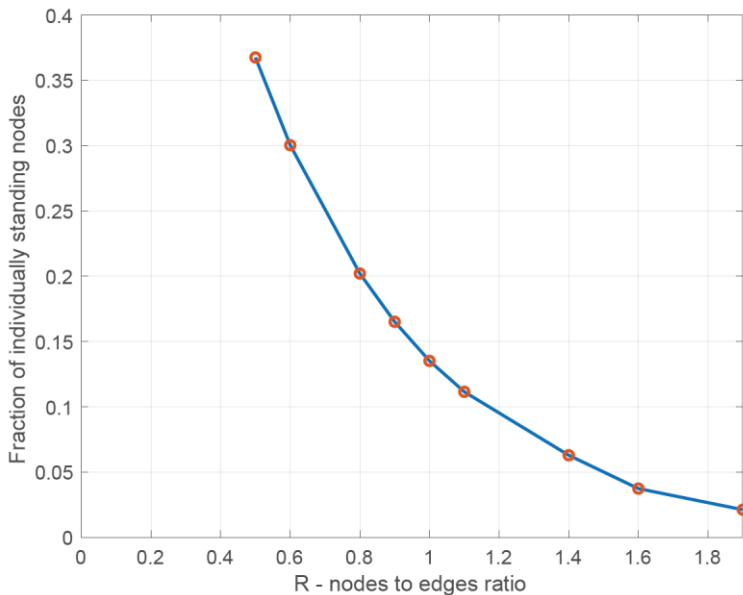


Fig.12. Experimental fraction of individually standing nodes in a graph $G(n,nR)$ as a function of the edges to nodes ratio R.

The experimental solution converges to a curve analytically derived from Erdős–Rényi graph model. A useful notation of a truly random graph according to Erdős–Rényi is the notation of $G(n, M)$, which represents a randomly selected graph G from set of all possible graphs with a number of nodes n and a number of nodes M . The order of the edges matters, two graphs obtained by a permutation of the other (replace two nodes one by the other) are distinct. There exist 3 possible graphs for a number of nodes $n = 2$ and a number of edges $e = 2$, as presented in (Fig.13). The selection for e edges is made from $K = \frac{n^2-n}{2}$ places, corresponding to the elements of the upper right triangle of the adjacency matrix $A(n)$, as that relates to undirected simple graphs.

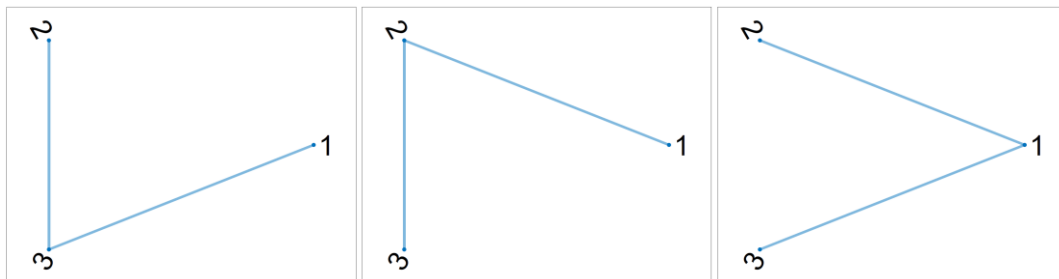


Fig.13. All Erdős–Rényi $G(3,2)$ model graphs.

Evaluating the equation (Eq.2) results in the number g of all possible graphs $G(n, M)$, that might incur using the number of nodes n and a number of edges e , where $M = e$.

$$g = \binom{K}{e} = \binom{\binom{n}{2}}{e} = \binom{n(n-1)/2}{e} \tag{2}$$

Similarly, the number of all possible graphs, which do have an isolated node is a function as per (Eq.3).

$$B_1 = \binom{\binom{n-1}{2}}{e} \tag{3}$$

The probability that the specific node is an individually standing 1-node component is modeled by (Eq.4).

$$P = \frac{B_1}{g} = \frac{\binom{\binom{n-1}{2}}{e}}{\binom{\binom{n}{2}}{e}} \tag{4}$$

The numerical computation of these double factorial equations for even small graphs reaches standard, computational memory limits quickly ($n = 170$)! = 7.2574E306 and a truncation rounding error ($n > 170$)! = ∞ . After research on the possibilities of working with very large numbers, an approach of analytical rearrangement was followed. An interesting equivalent mathematical notation was discovered by writing out the factors of the 2-level deep binomial coefficients. These product of series equations were found to be computationally more effective. Hence, the number of all possible Erdős–Rényi graphs that isolate a node becomes (Eq.6).

$$B_1 = \binom{\binom{n-1}{2}}{e} = \binom{\frac{n^2 - 3n + 2}{2}}{e} \tag{5}$$

$$= \frac{\frac{n^2 - 3n + 2}{2} \cdot \frac{n^2 - 3n + 2 - 2 \cdot 1}{2} \cdot \frac{n^2 - 3n + 2 - 2 \cdot 2}{2} \cdot \dots \cdot \frac{n^2 - 3n + 2 - 2(e-1)}{2} \cdot \frac{n^2 - 3n + 2 - 2e}{2}!}{\left(\frac{n^2 - 3n + 2}{2} - e\right)! \cdot e!}$$

$$= \prod_{a=0}^{e-1} \frac{n^2 - 3n + 2 - 2a}{2(a+1)} \tag{6}$$

And the number of all possible Erdős–Rény graphs is represented by (Eq.8):

$$g = \binom{\binom{n}{2}}{e} = \binom{\frac{n^2 - n}{2}}{e} \quad (7)$$

$$= \frac{\frac{n^2 - n}{2} \cdot \frac{n^2 - n - 2 \cdot 1}{2} \cdot \frac{n^2 - n - 2 \cdot 2}{2} \cdot \dots \cdot \frac{n^2 - n - 2(e-1)}{2} \cdot \frac{n^2 - n - 2e}{2}}{\left(\frac{n^2 - 3n + 2}{2} - e\right)! \cdot e!}$$

$$= \prod_{a=0}^{e-1} \frac{n^2 - n - 2a}{2(a+1)} \quad (8)$$

The difficulty now decreased to a product series equivalent of a single factorial calculation. Combining the (4), (6) and (8), the resulting probability of any node in randomly generated Erdős–Rényi graph is P in form of a product of series in Equation (9).

$$P = \frac{B_1}{g} = \frac{\binom{\binom{n-1}{2}}{e}}{\binom{\binom{n}{2}}{e}} = \prod_{a=0}^{e-1} \frac{n^2 - 3n + 2 - 2a}{n^2 - n - 2a} \quad (9)$$

Evaluating for $n = 120$ and $e = 60$, the ratio becomes $P = 36.33\%$. Similarly, for $n = 120$ and $e = 132$ the analytical expected value is $P = 10.65\%$, which when compared to the experimental value of 11.15% from the (Tab.4) above, represents a relative error 4.7% , upon the basis of the analytical. Similarly, evaluating Eq.(9) at $n = 3000$ a result of 0.1106 is obtained which results in a much smaller relative error of 0.81% .

Calculation for larger integers of number of nodes does yield in a much more stable, converging solution. The stability of the evaluation of equation (9) for nodes number $n = 1000$ through $n = 9000$ is presented in (Fig.14), where the curves for varying number of nodes are highly mutually congruent. The experimental values obtained by simulating a graph of 30000 nodes at a set of edges to nodes ratios also overlay the analytical solutions. In a semi-log figure, the curve becomes linear, which concludes in the fact, the fraction of the individually standing nodes (0-degree nodes) is an exponential function of the edges to nodes ratio.

$$\frac{n_{0\text{-degree}}}{n_{\text{ALL}}} \propto e^{-aR} \quad (10)$$

After model fit analysis, it was found that experimental values fit an exponential $a \cdot e^{bx}$ model with values of a and b 0.9993 and -2 respectively ($0.9775, 1.021$) and ($-2.031, -1.969$) within 95% confidence interval. This is an experimental proof, that the fraction of 0-degree nodes is in fact not only proportional as per equation (10) but equal to decaying exponential function of $2R$.

$$\frac{n_{0\text{-degree}}}{n_{\text{ALL}}} = e^{-2R} \quad (11)$$

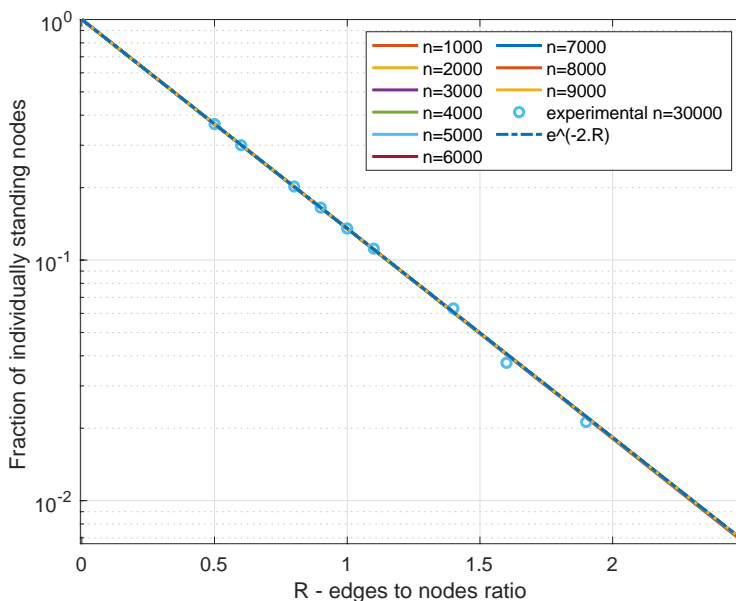


Fig.14. logY – Analytical results (curves) compared to the experimental results, based on Fig.12.

4 Node Degree Distribution Analysis

The next part of the analysis investigates the distribution of the number of nodes with respect to their neighbouring nodes, that is nodes in relation to respective degree numbers. Node degree histogram distributions were selected as a suitable methodology.

In this section, a randomly generated graph with a node number $n = 10000$ and initial number of edges to nodes ratio $R = 1.1$ is amended by the P-edge algorithm, such that nodes with a higher degree have got larger probability of gaining a new edge with any other node.

Histogram in (Fig.15) visualises the distribution of the number of closest neighbours (node degree number) for an initial, truly random graph. The distribution of such structure is binomial in essence.

The right-skewed distribution after adding 1000 P-edges is presented in (Fig.16). Following the algorithm, the distribution has skewed to the right, such that the average shifts to the higher node degrees and the actual magnitude decreases as the distribution spreads out. There are fewer nodes with low node degrees and more nodes with higher node degrees. The sum of the elements remains constant as the number of nodes does not change.

Analogously, after the addition of further 1000 P-edges, the distribution shifts again, the result of this intermediate step is presented in (Fig.17).

Another execution of the algorithm for extra 4000 P-edges resulted in a solution of a graph with initial number of nodes $n = 10000$ and a number of edges $e = 11000$, with additional 6000 P-edges, (Fig.18). The solution is equivalent to the process of generating 6000 P-edges for an initial graph at once, since the P-edge generation is iterative with associative property.

Conclusion is made, that the addition of P-edges to a graph expands the node degree count distribution and reduces the overall average count of nodes with a subjectively low node degree number and vice versa, best evidenced in 2-comparison distributions in (Fig.19). According to Blum et. al, the probability of any vertex having a degree less than a certain number decreases with any added edge in graph as a function of power law distribution (Blum et al. 2020).

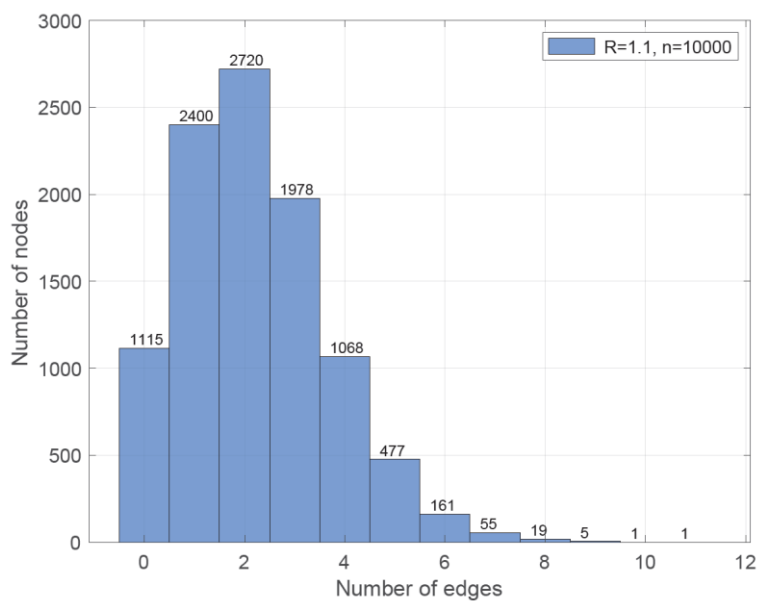


Fig.15. Node degree distribution for an initial graph, $n=10000$ and $e=11000$.

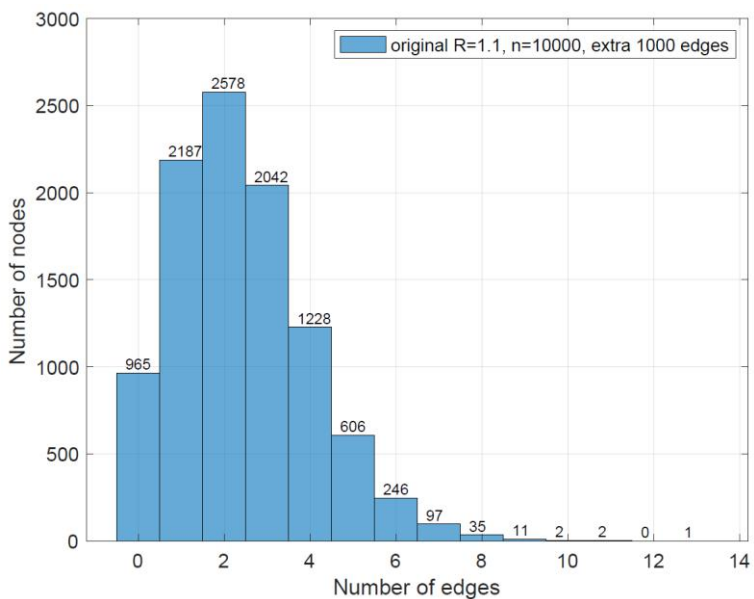


Fig.16. Node degree distribution for an initial graph, $n=10000$ and $e=11000$, with additional 1000 P-edges.

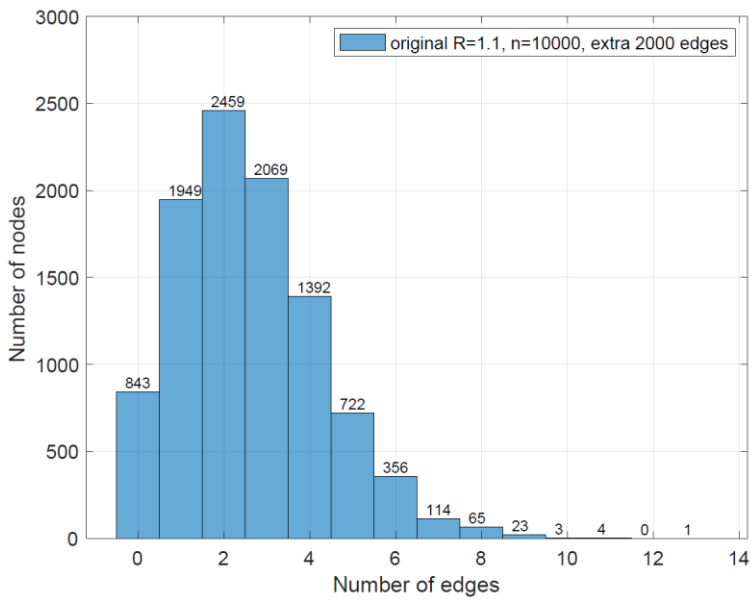


Fig.17. Node degree distribution for an initial graph, $n=10000$ and $e=11000$, with additional 2000 P-edges.

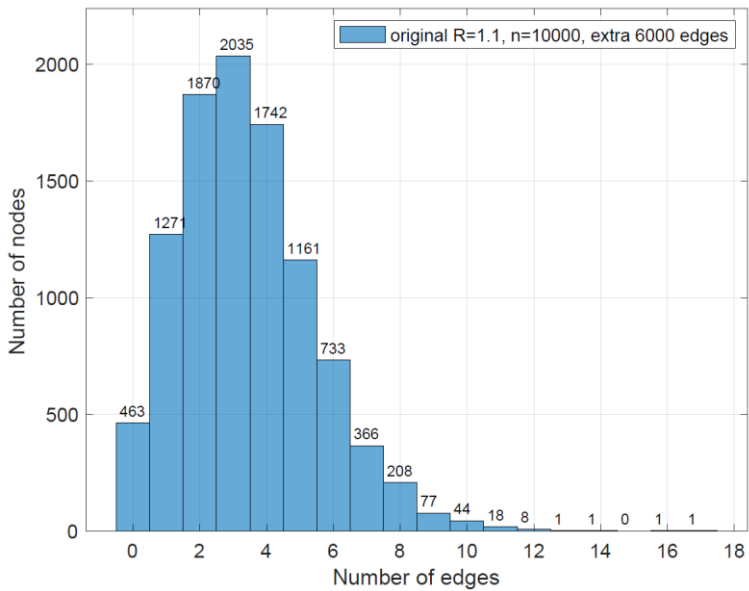


Fig.18. Node degree distribution for an initial graph, $n=10000$ and $e=11000$, with additional 6000 P-edges.

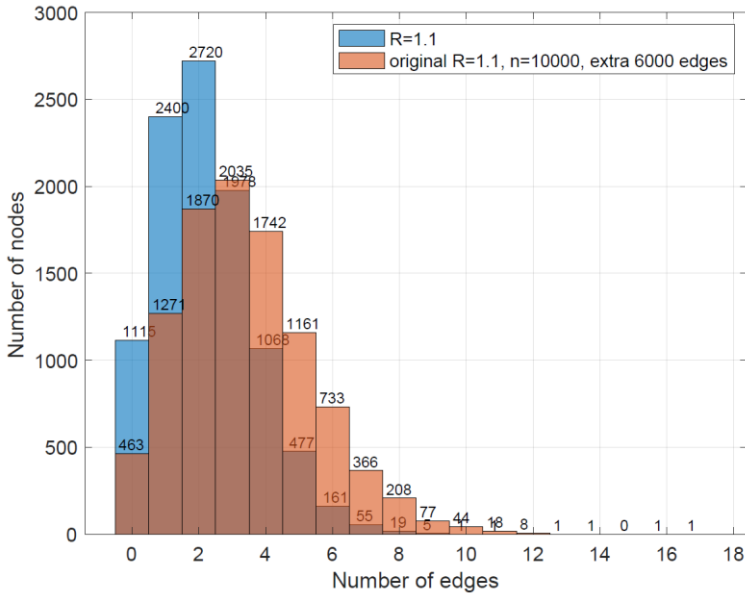


Fig.19. Comparison of the initial graph and a 6000 P-edge complemented graph, $n=10000$ and $e_1=11000$, $e_2=17000$ edges.

Conclusion

Custom random graph model and preferential edge attachment models were created and validated using the derived equations from graph theory. Several analytical features of complex networks were then experimentally confirmed. Linearly enlarged graphs with constant edges to nodes ratio render equivalent relative node degree distributions. Experimental fit of simulated random graphs presents a decaying exponential trend with respect to edges to nodes ratio. Preferential edge attachment percolation according to custom rules was simulated and analysed.

The approach of simulating quasi-static structured graph models will be expanded in future work, with focus on agent spreading in networks.

Acknowledgement

The baseline of these experiments was initially developed as a student assignment within the Modelling and Simulation module (Štefanovič, 2021). Subsequent work shall proceed with a bachelor thesis level project under the supervision of Juraj Štefanovič, at the Faculty of Informatics, Pan-European University in Bratislava, Slovakia.

References

- [1] Pelánek, R. (2011) *Simulace komplexních systémů*. (Simulation of Complex Systems), Masarykova univerzita, Brno, Czech Republic, ISBN: 9788021053182.
- [2] Štefanovič, J. (2021) Prednáška 4 - Vlastnosti komplexných sietí. (Lecture 4 - Features of Complex Networks), *the course: Modeling and Simulation*, Pan-European University, Bratislava, Slovakia.
- [3] Réka, A. and Barabási A.-L. (2002) Statistical mechanics of complex networks. Department of Physics, University of Notre Dame, *Reviews of Modern Physics*, Volume 74, pp. 47-97. <http://barabasi.com/publications/4/complex-networks>
- [4] Thulasiraman, K., Arumugam, S., Brandstädt, A., Nishizeki, T. (2016) Handbook of graph theory, combinatorial optimization, and algorithms. In: *Handbook of Graph Theory, Combinatorial Optimization, and Algorithms*, Chapman and Hall, doi: 10.1201/b19163.
- [5] Palko, V. (2017) *Diskrétna matematika pre informatikov*. (Discrete Mathematics for IT). OZ Hlbiny, ISBN: 9788089743247.
- [6] Blum, A., Hopcroft, J., Kannan, R. (2020) *Foundations of Data Science*. Cambridge University Press, ISBN: 9781108755528, doi: 10.1017/9781108755528.

Authors



MSc. David Šablatura

Student at the Faculty of Informatics, Pan-European University, Bratislava, Slovakia

sablatura.d@gmail.com

Completed his engineering studies at the University of Hertfordshire (Aerospace technology with pilot studies, BSc) and Cranfield University (Aerospace Dynamics, MSc), with individual projects on bird wing aerodynamics with numerical-empirical approach and an analytic study of hydrofoil stability. Studying at the Faculty of Informatics, he is currently focused on modelling and simulation from applied informatics perspective.

MODEL PREDICTIVE CONTROL - APPLICATION FOR PHYSICAL MODEL

Štefan Kozák

Abstract:

Paper deals with the one of effective application of MPC control for a laboratory thermal-optical system. Laboratory model is realized by two channels: thermal channel and optical channel and their dynamical mathematical models can be described by a step-response model. The main goal of the proposed paper is design and application of the modified constrained dynamic matrix control algorithm for the considered laboratory process with supporting of Matlab-Simulink. Proposed and implemented dynamic matrix control algorithm is compared with conventional PID algorithm. Final part of paper deals with possible implementation of MPC for FPGA hardware realization.

Keywords:

Dynamic model, prediction, predictive control, optimization, process control.

ACM Computing Classification System:

Physical sciences and engineering, automatic control, integrated circuits.

Introduction

Predictive control has become popular over the past twenty years as a powerful tool in feedback control for solving many problems for which other control approaches have been proved to be ineffective. Predictive control is a control strategy that is based on the prediction of the plant output over the extended horizon in the future [13] which enables the controller to predict future changes of the measurement signal and to base control actions on the prediction.

Model predictive control (MPC) refers to a class of control algorithms that compute a sequence of control inputs based on an explicit prediction of outputs within some future horizon. The computed control inputs are typically implemented in a receding horizon fashion, meaning only the inputs for the current time are implemented and the whole calculation is repeated at the next sampling time. Therefore, one of the most important strengths of MPC is that it can consider the constraints of input and output variables that often exist in real industrial systems.

One of the most well-known MPC algorithms for the process control is dynamic matrix control (DMC), which assumes a step-response model (SRM) for the underlying system.

Predictive control has many advantages. Due to them, the predictive control approach has many applications. Examples include medical applications, civil engineering applications, and mechanical engineering applications as well as chemical and petrochemical engineering applications. A survey of industrial model predictive control technology is provided in many publications [9].

The paper is organized as follows. First, basic principles of predictive control and design of dynamic matrix controller are introduced in Section 1. Then, the laboratory thermal-optical system and identification of are described in Section 2. The experimental result from the testing of modified and designed DMC controllers are shown in Section 3 – experimental results. FPGA realization of MPC algorithm are described in Section 4. Summary and conclusions are given in last Section.

1 Dynamic Matrix Control

A Basic principles of predictive algorithms

Basic principles of predictive control [8]:

- specifying reference trajectory $y_{ref}=w(k)$ and its prediction on the chosen horizon of prediction p (Fig.1)
- prediction of a plant output on the predefined time horizon ($N = k + i$), i.e. prediction of $\hat{y}(k + i)$ for $i = 1, \dots, p$ (p is the prediction horizon length) in discrete steps based on real values of control input in the past steps $u(k + i)$ for $i = 0, \dots, m-1$ (where $m < p$ is the length of the control horizon)
- computation of new control input based on the knowledge of the mathematical model and optimal cost index J
- minimization of cost and computation of control input which ensures that the predicted output tracks the reference trajectory
- correction of the prediction function error between measured and predicted variable.

The three basic elements of predictive control are the model, which describes the process, the goal defined by an objective function and constraints, and the optimization procedure. Parameters chosen by users are the prediction horizon, control horizon, parameters in the objective function and constraints.

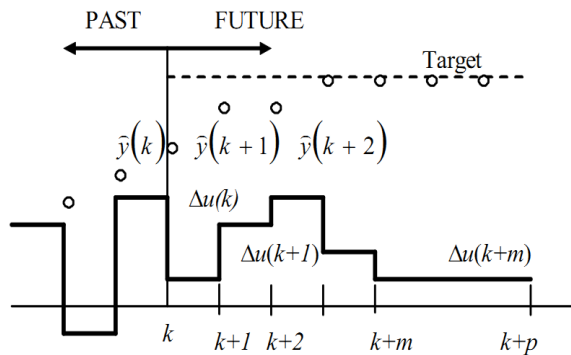


Fig.1. Basic principles of predictive algorithm.

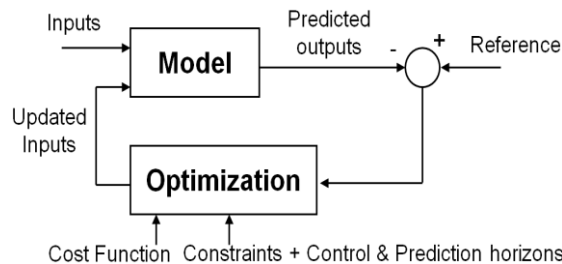


Fig.2. Block scheme of Model Predictive Control (MPC).

Process interactions and deadtimes can be intrinsically handled by model predictive control schemes such as dynamic matrix control (DMC).

The sequence of future control signals is computed by optimizing a given cost function [5].

B Design of dynamic matrix control

In 1979, Cutler and Ramaker of Shell oil Co. presented details of an unconstrained multivariable control algorithm, which they named Dynamic Matrix Control (DMC) [9]. It is evolved from a technique of representing process dynamics with a set of numerical coefficients [3].

The Dynamic matrix is used for projecting the future outputs. It is suitable for linear open loop stable process. The DMC technique is based on a step response model of the process.

The objective of the DMC controller is to drive the output to track the set point in the least squares sense including a penalty term on the input moves. This results in smaller computed input moves and a less aggressive output response [9].

Consider the single input single output (SISO) case, the step response model of the plant,

$$y(t) = \sum_{i=1}^{\infty} g_i \Delta u(t - i) \quad (1)$$

The disturbance at instant t along the horizon is,

$$\hat{x}(t + j/t) = \hat{x}(t/t) = e(t) \quad (2)$$

$$e(t) = y_m(t) - \hat{y}(t/t) \quad (3)$$

The predicted value along the horizon will be:

$$\hat{y}(t + j/t) = \sum_{i=1}^{\infty} g_i \Delta u(t + j - i) + \hat{x}(t + j/t) \quad (4)$$

For constant disturbance the predicted value of output is,

$$\hat{y}(t + j/t) = \sum_{i=1}^j g_i \Delta u(t + j - i) + f(t + j) \quad (5)$$

The second term of equation (5) is the free response, which does not depend on the future control actions. The prediction along the prediction horizon p and m control actions (j=1, ..., p) is [2]:

$$\hat{y}(t + p/t) = \sum_{i=1}^p g_i \Delta u(t + p - i) + f(t + p) \quad (6)$$

Equation (5) can be written as,

$$\hat{y} = Gu + f \quad (7)$$

Equation (7) shows the relation between future output and control increments.

$$G = \begin{bmatrix} g_1 & 0 & \dots & 0 \\ g_2 & g_1 & \dots & 0 \\ \vdots & \vdots & \ddots & \vdots \\ g_m & g_{m-1} & \dots & g_1 \\ \vdots & \vdots & \ddots & \vdots \\ g_p & g_{p-1} & \dots & g_{p-m+1} \end{bmatrix} \quad (8)$$

The systems dynamic matrix G is made up of m (the control horizon) columns of the systems step response appropriately shifted down in order.

The predicted output with disturbances is,

$$\hat{y}_d = G_d u_d + f_d \quad (9)$$

The cost function to be minimized including control effort is [10],

$$J = \sum_{N_1}^{N_2} \delta(j) [\hat{y}(t + j/t) - w(t + j)]^2 + \sum_{N_1}^{N_2} \lambda(j) [\Delta u(t + j - 1)]^2 \quad (10)$$

Without constraints, cost functions is

$$J = ee^T + \lambda uu^T \quad (11)$$

The solution to this cost function can be obtained by computing the derivative of J and equating it to zero

$$u = (G^T G + \lambda I)^{-1} G^T (w - f) \quad (12)$$

In DMC control horizon and penalization factor are the tuning parameter. In least square formulation penalization factor is introduced to smoothen the control signal [4].

Standard QP at each sampling instant carries out the optimization. According to receding horizon concept, at time t, only the first input ($\Delta u(t)$) of the vector of future control increment or sequence (u) is actually applied to the plant. The remaining optimal inputs are discarded, and a new optimal control problem is solved at time t + 1[1].

When constraints are considered in input and output, the following equation must be added to the minimization [5], (i = 1, ..., Nc):

$$\sum_{j=1}^N c_{yj}^i \hat{y}(t + j/t) + c_{uj}^i u(t + j - 1) + c^i \leq 0 \quad (13)$$

In DMC, the design of control is independent of the transport lag and it deals with constraints. In presence of disturbances, feed-forward can be easily implemented. It is robust to model error but the application is limited to open loop bounded input bounded output (BIBO) stable type of processes [6], [7]. For DMC algorithm to be closed loop stable, a long length of prediction horizon is required [9].

2 Thermal-Optical System

A Description of the thermal-optical system

The thermal-optical system uDAQ28 L/T (Fig. 3) is an experimental laboratory device aimed primarily for education of automatic control. The device allows for real time measurement and control of temperature and light intensity.

It can be connected to a computer via a universal serial bus and communication with Matlab environment is fully supported. It is multivariable system with three manipulated inputs and eight measured outputs.

System has three manipulated inputs: bulb voltage (0-5V) which represents heater and light source, fan voltage (0-5V) which can be used for temperature decreasing and voltage of led diode (0-5V) which represents another source of light.

On the output of the system is possible to measure seven variables: temperature insight the system (direct or filtrated), outisght temperature, light intensity (direct or filtrated), fan velocity and fan current.

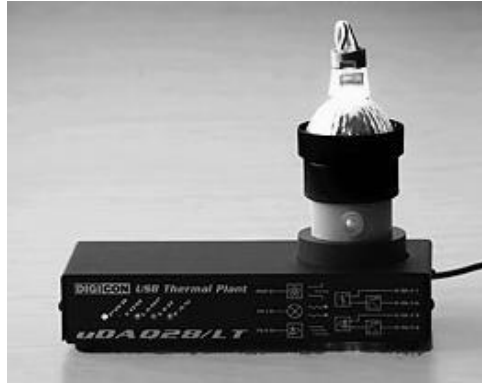


Fig.3. Front view on the thermal-optical system.

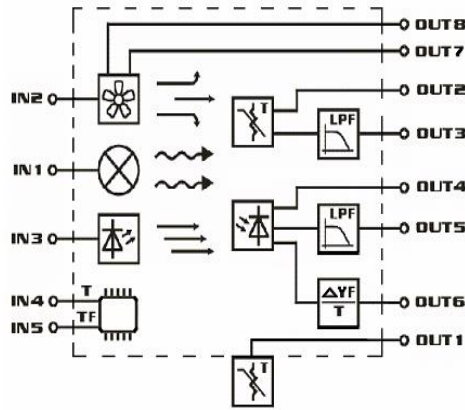


Fig.4. Structure of the thermal-optical system.

B Light intensity identification

The dynamics of the light intensity channel of the measured thermal-optical system can be determined from the response of the process to steps deterministic signal. The two-point algorithm approach was given for the process identification.

The step response of the light intensity channel has typical first-order characteristic with transport delay time constant.

$$G(s) = \frac{K_r}{T_p s + 1} e^{-Ds} \quad (14)$$

The process gain is determined by dividing of the steady state output by the input set-point value. The time taken for the process output to reach 33% and 70% of the final steady state output is used to determine the time constant and the dead time based on solving the following simultaneous equations:

$$T_p = 1.245(t_{0.7} - t_{0.33}) \quad (15)$$

$$D = 1.498t_{0.33} - 0.498t_{0.7} \quad (16)$$

The process gain and time constant was given from step response characteristics:

$$t_{0.33} = 0.558s, t_{0.7} = 0.398s, K_r = 4.103 \quad (17)$$

Substituting these measured coefficients in relations (15) and (16) are obtaining the transfer function parameters of the identified model

$$G(s) = \frac{4.103}{0.1992s+1} e^{-0.3183s} \quad (18)$$

The step responses of the compared identified first-order model and measured laboratory system are shown in (Fig.5).

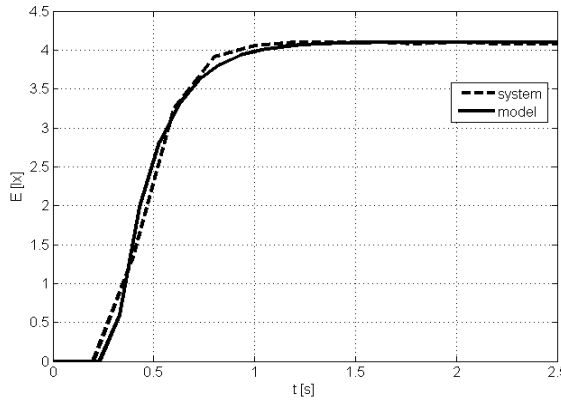


Fig.5. Step responses of the compared identified model and measured thermal-optical system.

3 Experimental Results

DMC control algorithm of the light intensity of the thermo-optical system was written in MATLAB. Figure 7 shows the DMC response of light intensity for a step change 10 in the set point of the. The result shows that DMC control the light intensity in the presence of set point change. The value of the controls horizon were taken 1, 2 and prediction horizon were taken as 10 and 20. A sampling interval of 0.1 second was chosen. DMC brings and maintains the controlled variable around the set point after some time.

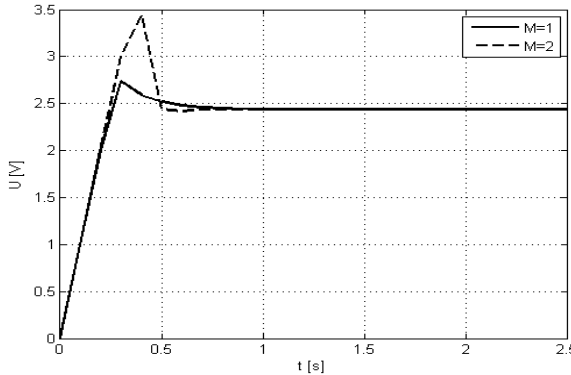


Fig.6. Time responses of the manipulated variables of two compared DMC controllers [12].

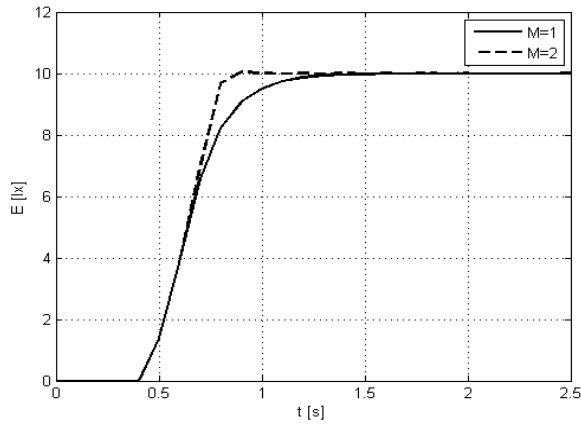


Fig.7. Time responses of the controlled variables of two compared DMC controllers [12].

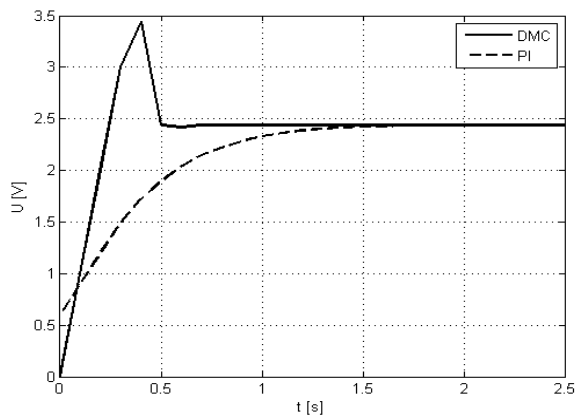


Fig.8. Time responses of the manipulated variables of DMC and PI controllers [12].

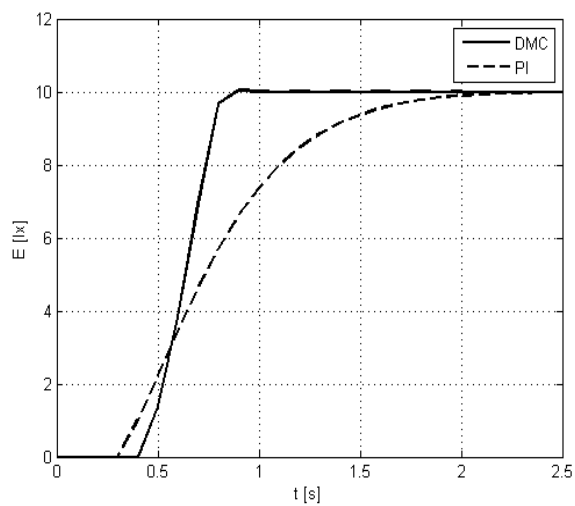


Fig.9. Time responses of the controlled variables two compared controllers, DMC and PI controller [12]

The comparison of designed DMC controller with conventional PI controller are shown in the figures on previous page. The parameters of the PI controller were designed on the base of the identified first-order model.

4 FPGA MPC Realization

The main factors to be considered when implementing MPC on reconfigurable hardware include computational speed, hardware resource usage. For a particular application, specific requirements on these factors need to be met and the final implementation is usually a compromise between all these factors. Hence, an effective and efficient rapid prototyping environment which allows for experimentation and verification of various algorithm configurations, architecture and implementation schemes would be useful [11].

The tools used in this study include a Xilinx Spartan-3A Starter Kit, the Xilinx ISE Design Suite and MATLAB/Simulink software. The Xilinx Spartan 3-A Starter Kit is a platform for evaluation and development of FPGA based applications. The platform includes a Xilinx Spartan-3A FPGA, external memory, programmable clocks, A/D and D/A converters, Ethernet, RS-232 port, etc. The core of Spartan-3A (Fig.11) development board is a Xilinx Spartan-3A FPGA chip which has 1.5 million logic gates and some useful on-chip resources such as multiplier and on-chip memory. Xilinx ISE design suite is an integrated environment for FPGA implementation. It provides a complete tool set which includes a compiler, a debugger, an optimizer and a simulator. MPC algorithm design and simulation,

MATLAB/Simulink provides an excellent platform for plant modeling, MPC algorithm design and simulation, Handel-C/MATLAB co-simulation and hardware-in-the-loop verification. Handel-C is a high-level FPGA implementation language with an ANSI C syntax and some hardware related language features such as parallel execution, channel communication, interface definition, etc. Compared with other hardware description languages such as VHDL, Handel-C is more convenient for rapid prototyping of MPC control algorithms.

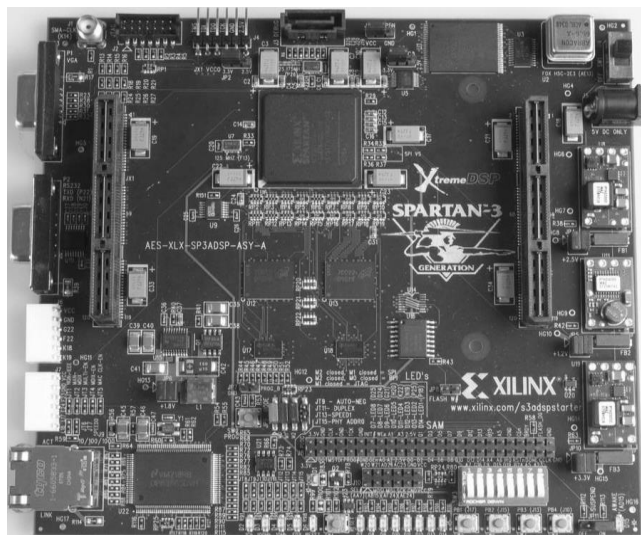


Fig.11. Xilinx Spartan-3A development board.

The main procedure of prototyping of our MPC algorithm on FPGA design is illustrated in (Fig.12).

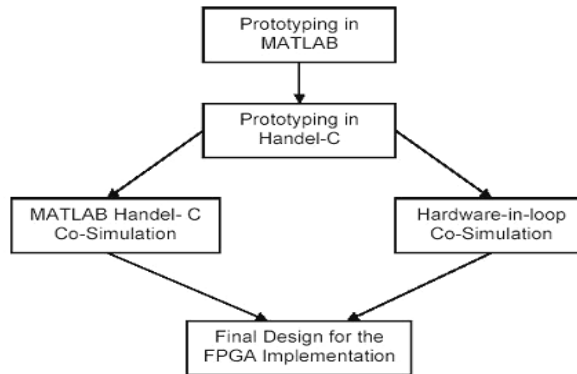


Fig.12. Prototyping of MPC control system [11].

In the following part we briefly describe the main steps in prototyping MPC into a FPGA implementation.

- Prototyping in MATLAB provides an excellent computation and simulation environment for designing and implementing control algorithms. The MPC algorithm is first prototyped in MATLAB code and then simulated and verified in the MATLAB/Simulink environment.
- Prototyping in Handel-C code, the prototype MPC in the form of MATLAB code is translated into Handel-C code for FPGA realization. It is mapped, placed and routed by Xilinx ISE to a target FPGA. The Xilinx tool would report hardware resource usage and timing performance. If the results do not meet the specified requirements, design iterations would need to be carried out.
- Handel-C/MATLAB co-simulation, two options are available for algorithm verification: software or hardware verification. For software verification, the Handel-C code will be packaged into a DLL file and then be called by Simulink as a S-function.
- Hardware-in-the-loop verification, for hardware verification, the Handel-C code will be compiled into a bitstream file which will subsequently be down-loaded onto the FPGA on the Spartan-3A development board to perform the MPC calculations. A test suite can then be written to verify the MPC implementation on the FPGA.

Conclusion

In this paper the modification and design of dynamic matrix controller for laboratory thermo-optical system has been designed and verified on light intensity channel of the measured system. The verification of designed dynamic matrix controller was provided on test with conventional proportional integral controller. The result from the verification of the designed dynamic matrix controller in terms of performance for the identified model of the optical channel was very good. Currently we develop and verified different predictive methods by FPGA realisation and we would like to compare them with conventional model predictive control algorithm for fast processes.

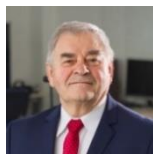
Acknowledgement

This paper has been supported by the Slovak Scientific Grant Agency, Grant No. 1/1105/11.

References

- [1] A. Bemporad, M. Morari (1999) Model Predictive Control: A Survey, *Robustness in identification and control*, vol. 245.
- [2] E.F.Camacho, C. Bordons (2004) *Model Predictive Control*, Springer, London.
- [3] C.R. Cutler, B. Ramaker (1980) Dynamic Matrix Control - A computer control Algorithm, *Proceedings of the 1980 Joint Automatic Control Conference*, vol. WP5-13.
- [4] R.M.C. De Keyser, PH.G.A. Van De Velde (1988) A comparative Study of Self-adaptive Long range Predictive Control Methods, *Automatica*, vol. 24, no. 2, pp. 149-163.
- [5] C.E. Garcia, D.M. Prett, M. Morari (1989) Model Predictive Control: Theory and Practice a Survey, *Automatica*, vol. 25, no. 3, pp. 335-348.
- [6] J.C. Hung (1996) *Practical techniques for industrial control*, IEEE, pp. 5-10.
- [7] P. Lundstrom, J.H. Lee, M.M.(1999) S.S. Limitations of DMC, *Computers Chem. Eng.*, vol 19, no 4, pp. 409-421.
- [8] J.A. Roubos, S. Molloy, R. Babuska, H.B. Verbruggen (1999) Fuzzy model-based predictive control using Takagi-Sugeno models, *International Journal of Approximate Reasoning* 22, pp. 3-30.
- [9] S.J. Quin, T.A. Badgwell (2003) A survey of industrial model predictive control technology, *Control Engineering Practice*, vol. 11, pp. 733-764.
- [10] Xie, K. Sang, J.T.Y. Lin (1997) A New Dynamic Matrix Control Algorithm Based on the FNN TS Fuzzy Model, IEEE International Conference on Intelligent Processing Systems, pp. 317-321.
- [11] K.V. Ling, S.P. Yue and J.M. Mackiejowski (2011) A FPGA Implementation od Model Predictive Control, *IFAC World Congress*, vol. 18, Milano, pp. 1930-1935.
- [12] P. Guzmický, Kozák Š. (2012) Dynamic matrix control of thermal-optical laboratory system, *Portuguese Conference on Automatic Control – CONTROLO*, vol. 10, Madeira.
- [13] C. Georgescu, A. Afshari and G. Bornard (1993) Fuzzy predictive PID controllers: An heating control application, *2th IEEE Conference on Fuzzy System*, pp. 1091-1098.

Authors



prof. Ing. Štefan Kozák, PhD.

Faculty of Informatics, Pan-European University, Bratislava, Slovakia
 stefan.kozak@paneurouni.com

Currently at the Institute of Applied Informatics at the Faculty of Informatics, Pan-European University in Bratislava. His research interests include system theory, linear and nonlinear control methods, numerical methods and software for modeling, control, signal processing, IoT, IIoT and embedded intelligent systems for digital factory in automotive industry.

List of Reviewers

Issue 1/2021, in alphabetic order

Cigánek, J. - Slovak University of Technology in Bratislava, Slovakia

Haffner, O. - Slovak University of Technology in Bratislava, Slovakia

Képešiová, Z. - Slovak University of Technology in Bratislava, Slovakia

Kozáková, A. - Slovak University of Technology in Bratislava, Slovakia

Kučera, E. - Slovak University of Technology in Bratislava, Slovakia

Rosinová, D. - Slovak University of Technology in Bratislava, Slovakia

Lacko, J. - Pan-European University, Bratislava, Slovakia



INDUCTOR ENERGY

Q 1 0 D1 90

L 1 2 200MH IC=0

R 2 0 5 0 SMOD

D 2 3 DMOD

R 3 1 20

VCONTROL 5 0 PULSE(-10 10 0 10N 10N 10MS 100MS)

TRAN 1M 100MS 0 .1M UIC

voltage-controlled switch

control for switch
falling time of 0.1 ms
gives smooth traces

switch model, on
resistance set to .001
default diode model